High energy cosmic rays from decaying supersymmetric Dark Matter

JHEP05(2009)110

(http://iopscience.iop.org/1126-6708/2009/05/110)

JHEP

Published by IOP Publishing for SISSA

Received: *March 10, 2009*
Revised: *April 14, 2009*
Accepted: *April 29, 2009*
Published: *May 26, 2009*

JHEP05(2009)110

High energy cosmic rays from decaying supersymmetric Dark Matter

Koji Ishiwata,[a] **Shigeki Matsumoto**[b] **and Takeo Moroi**[a]

[a] *Department of Physics, Tohoku University, Sendai 980-8578, Japan*
[b] *Department of Physics, University of Toyama, Toyama 930-8555, Japan*
E-mail: ishiwata@tuhep.phys.tohoku.ac.jp, smatsu@sci.u-toyama.ac.jp, moroi@tuhep.phys.tohoku.ac.jp

Abstract: Motivated by the recent PAMELA and ATIC results, we calculate the electron and positron fluxes from the decay of lightest-superparticle (LSP) dark matter. We assume that the LSP is the dominant component of dark matter, and consider the case that the R-parity is very weakly violated so that the lifetime of the LSP becomes of the order of 10^{26} sec. We will see that, with such a choice of the lifetime, the cosmic-ray electron and positron from the decay can be the source of the anomalous $e^{\pm}$ fluxes observed by PAMELA and ATIC. We consider the possibilities that the LSP is the gravitino, the lightest neutralino, and scalar neutrino, and discuss how the resultant fluxes depend on the dark-matter model. We also discuss the fluxes of γ-ray and anti-proton, and show that those fluxes can be consistent with the observed value in the parameter region where the PAMELA and ATIC anomalies are explained.

Keywords: Supersymmetry Phenomenology

ArXiv ePrint: 0903.0242

doi:10.1088/1126-6708/2009/05/110

Contents

1 Introduction **1**

2 Basic setup **2**
- 2.1 Sources of the cosmic rays 3
- 2.2 Electron & positron fluxes 3
- 2.3 Anti-proton flux 5
- 2.4 γ-ray flux 5

3 Gravitino LSP **6**

4 Neutralino LSP **16**

5 Sneutrino LSP **21**

6 Conclusions and discussion **23**

A Green's function **26**

JHEP05(2009)110

1 Introduction

In astrophysics, the existence of dark matter is almost conclusive. According to the recent survey of WMAP [1], it accounts for 23 % of the total energy density in the universe. In the standard model of particle physics, however, there does not exist candidate for dark matter, which is one of the reasons to call for new physics beyond the standard model. Supersymmetry (SUSY) is a promising model which can give an answer to the question; in the framework of SUSY, lightest superparticle (LSP) is a viable candidate for dark matter.

The fluxes of high energy cosmic rays give information about the properties of dark matter. In the recent years, accuracy of the measurements of the fluxes have been significantly improved. In particular, anomalous signals are reported by PAMELA [2] and ATIC [3] in the observations of high energy cosmic-ray positron and electron. The PAMELA and ATIC results have attracted many attentions because the anomalies may indicate an unconventional nature of dark matter. In fact, a sizable number of dark-matter models are proposed to explain the anomalies after the announcements of the PAMELA and ATIC results. Roughly speaking, the possibilities to produce such high energy electron and positron are categorized into two: the decay and the annihilation of dark matter.[1] (For early attempts to calulate the spectra of cosmic-ray $e^{\pm}$, see [5–21] and [7, 22–31] for decaying and

[1]The other possibilities to enhance the $e^{\pm}$ fluxes considered using nearby pulsars [4].

annihilating dark matter, respectively.) In general, the latter case has the difficulty to reproduce the anomalous cosmic-ray positron and electron fluxes without large enhancement factor, called boost factor.[2] In the former case, on the other hand, the observed anomalies can be well explained with the appropriate choice of the lifetime of dark matter especially in leptonically decaying scenarios.

In usual supersymmetric scenario, R-parity conservation is assumed, which protects LSP from decaying into standard model particles and makes it a viable candidate for dark matter. If we consider the case that R-parity is violated, LSP is no loner stable; however, if R-parity violation (RPV) is weak enough, the lifetime of the LSP can be much longer than the present age of the universe and LSP can play the role of dark matter [34]. In addition, when the size of the RPV is properly chosen to give the lifetime of $O(10^{26}$ sec), produced cosmic-ray positron gives excellent agreement with PAMELA data [7].

In this paper, we calculate fluxes of cosmic-ray positron, electron, γ-ray, and anti-proton in various LSP dark matter scenarios, paying particular attentions to the results given by PAMELA and ATIC. We consider the cases where the LSP dark matter is unstable, assuming that R-parity is (very weakly) violated. Then, we compare the calculated fluxes with the results of observations. We will see that the PAMELA and ATIC anomalies are simultaneously explained if the lifetime of the LSP dark matter is $O(10^{26}$ sec) and the mass is $\sim 1-1.5$ TeV. In addition, in some cases, γ-ray and anti-proton are also produced by the decay of the LSP. We will see that, taking account of the uncertainties in the Galaxy and propagation models as well as the error in the observations, the scenarios are not excluded by the observations of γ-ray and anti-proton fluxes yet.

The organization of this paper is as follows. In the next section, we explain the basic procedures to calculate the high energy cosmic-ray fluxes. Then, we discuss the cosmic-ray fluxes for the cases where the LSP is the gravitino, the lightest neutralino, and the sneutrino in sections 3, 4, and 5, respectively. Section 6 is devoted for conclusions and discussion.

2 Basic setup

As we have discussed in introduction, we consider the case where the LSP is unstable and has lifetime much longer than the present age of the universe so that most of the LSPs produced in the early universe survive until today. Then, if the relic density of the LSP is right amount, the LSP can be dark matter. In such a case, the LSP dark matter becomes the source of high energy cosmic rays.

The fluxes of the cosmic rays from the decay of the relic LSP depends on what the LSP is, and how the LSP decays. The LSP should be an electrically neutral particle and we consider the following three important cases:

- Gravitino LSP
- Neutralino LSP
- Sneutrino LSP

[2]However, cosmic-ray $e^{\pm}$ fluxes may be enhanced without large boost factor with the Breit-Wigner enhancement of the annihilation cross section [31], Sommerfelt enhancement [32], or with a nearby clump of dark matter [33].

JHEP05(2009)110

In addition, we adopt R-parity violation so that the LSP becomes unstable. Then, the lifetime of the LSP becomes longer as the coupling constants for the RPV interactions become smaller. We therefore treat the lifetime of the LSP as a free parameter in the following analysis. To be specific, we assume that the R-parity violation is so weak that the lifetime of the LSP becomes much longer than the present cosmic time.

2.1 Sources of the cosmic rays

With the decay of relic LSP, energetic particles (in particular, γ, $e^{\pm}$, and anti-proton $\bar{p}$) are produced. The production rate of the energetic particle I is given by

$$Q_I(E,\vec{x}) = \frac{1}{\tau_{\rm LSP}} n_{\rm LSP}(\vec{x}) \left[\frac{dN_I}{dE}\right]_{\rm dec}, \tag{2.1}$$

where $[dN_I/dE]_{\rm dec}$ is the energy distribution of particle I from the single LSP decay process. We have used the PYTHIA package [35] to calculate $[dN_I/dE]_{\rm dec}$. In addition, $\tau_{\rm LSP}$ and $n_{\rm LSP}$ are the lifetime and number density of the LSP at the present universe, respectively. In the calculation of the cosmic-ray spectrum, the origin of the dark-matter LSP is unimportant. Even though it is often assumed that the relic density of the LSP is thermally determined, non-thermal production of the LSP dark matter is also possible [36]. We thus do not specify the origin of the relic LSP in the following analysis, and set $n_{\rm LSP}$ to be $\Omega_{\rm LSP} = \Omega_{\rm DM}$, where $\Omega_{\rm LSP}$ and $\Omega_{\rm DM}$ are the density parameters of the LSP and dark matter, respectively.[3] Then, the mass density of dark matter is given by $\rho_{\rm DM}(\vec{x}) = m_{\rm LSP} n_{\rm LSP}(\vec{x})$. In calculating the fluxes of high-energy cosmic rays, we adopt the Navarro-Frank-White (NFW) mass density profile [37]:

$$\rho_{\rm NFW}(\vec{x}) = \rho_\odot \frac{r_\odot (r_c + r_\odot)^2}{r (r_c + r)^2}, \tag{2.2}$$

where $\rho_\odot \simeq 0.30$ GeV/cm^3 is the local halo density around the solar system, $r_c \simeq 20$ kpc is the core radius of the dark matter profile, $r_\odot \simeq 8.5$ kpc is the distance between the Galactic center and the solar system, and r is the distance from the Galactic center. Using the Q_I given in eq. (2.1) as a source term, we solve the propagation equations for individual particles. The diffusion zone is approximated as a cylinder with half-height L and radius $R = 20$ kpc.

2.2 Electron & positron fluxes

In order to calculate the fluxes of electron and positron from the LSP decay, we derive a static solution of the following diffusion equation:

$$\frac{\partial f_{e^\pm}(E,\vec{x})}{\partial t} = K_{e^\pm}(E)\nabla^2 f_{e^\pm}(E,\vec{x}) + \frac{\partial}{\partial E}\left[b(E) f_{e^\pm}(E,\vec{x})\right] + Q_{e^\pm}(E,\vec{x}), \tag{2.3}$$

with the condition $f_{e^\pm} = 0$ at the boundary of the diffusion zone, where $f_{e^\pm}$ is the number density of $e^\pm$ per unit energy. Our basic procedure to solve the diffusion equation (2.3) is explained in appendix A.

[3] Even if $\Omega_{\rm LSP} < \Omega_{\rm DM}$, the relic LSP can still be the source of high energy cosmic rays. Then, the fluxes can be obtained by rescaling the lifetime as $\tau_{\rm LSP} \to (\Omega_{\rm LSP}/\Omega_{\rm DM})\tau_{\rm LSP}$.

JHEP05(2009)110

	M1	MED	M2
L [kpc]	15	4	1
δ	0.46	0.70	0.55
$K_{e^\pm}^{(0)}$ [kpc^2/Myr]	0.0765	0.0112	0.00595

Table 1. Parameter sets for the propagation model of $e^\pm$.

We approximate the function $K_{e^\pm}$ as [38]

$$K_{e^\pm} = K_{e^\pm}^{(0)} E_{\rm GeV}^{\delta}, \tag{2.4}$$

with $E_{\rm GeV}$ being energy in units of GeV, while the energy-loss rate b is given by

$$b = 1.0 \times 10^{-16} E_{\rm GeV}^2 \ {\rm GeV/sec}. \tag{2.5}$$

We adopt three sets of diffusion parameters, which are summarized in table 1. The MED set gives the best-fit value in the boron-to-carbon ratio (B/C) analysis, while the maximal and minimal positron fractions are expected in the M1 and M2 sets without conflicting the B/C analysis.

Once $f_{e^\pm}$ are given by solving the above equation, the fluxes can be obtained as

$$[\Phi_{e^\pm}(E)]_{\rm DM} = \frac{c}{4\pi} f_{e^\pm}(E, \vec{x}_\odot), \tag{2.6}$$

where $\vec{x}_\odot$ is the location of the solar system, and c is the speed of light. In order to calculate the total fluxes of $e^\pm$, we also have to estimate the background fluxes. In our study, we adopt the following fluxes for cosmic-ray electrons and positrons produced by collisions between primary protons and interstellar medium in our galaxy [39]:

$$[\Phi_{e^-}]_{\rm prim} = \frac{0.16 E_{\rm GeV}^{-1.1}}{1 + 11 E_{\rm GeV}^{0.9} + 3.2 E_{\rm GeV}^{2.15}} ({\rm GeV\ cm^2\ sec\ str})^{-1}, \tag{2.7}$$

$$[\Phi_{e^-}]_{\rm sec} = \frac{0.70 E_{\rm GeV}^{0.7}}{1 + 110 E_{\rm GeV}^{1.5} + 600 E_{\rm GeV}^{2.9} + 580 E_{\rm GeV}^{4.2}} ({\rm GeV\ cm^2\ sec\ str})^{-1}, \tag{2.8}$$

$$[\Phi_{e^+}]_{\rm sec} = \frac{4.5 E_{\rm GeV}^{0.7}}{1 + 650 E_{\rm GeV}^{2.3} + 1500 E_{\rm GeV}^{4.2}} ({\rm GeV\ cm^2\ sec\ str})^{-1}. \tag{2.9}$$

With these backgrounds, the total fluxes are obtained as

$$[\Phi_{e^+}]_{\rm tot} = [\Phi_{e^+}]_{\rm DM} + [\Phi_{e^+}]_{\rm sec}\,, \tag{2.10}$$

$$[\Phi_{e^-}]_{\rm tot} = [\Phi_{e^-}]_{\rm DM} + [\Phi_{e^-}]_{\rm prim} + [\Phi_{e^-}]_{\rm sec}\,. \tag{2.11}$$

Using the fluxes defined above, the positron fraction, which is measured by the PAMELA, is defined as

$$R_{e^+} = \frac{[\Phi_{e^+}(E)]_{\rm tot}}{[\Phi_{e^-}(E)]_{\rm tot} + [\Phi_{e^+}(E)]_{\rm tot}}. \tag{2.12}$$

JHEP05(2009)110

	MAX	MED	MIN
L [kpc]	15	4	1
δ	0.46	0.70	0.85
$K_{\bar{p}}^{(0)}$ [kpc^2/Myr]	0.0765	0.0112	0.0016
V_c [km/s]	5	12	13.5

Table 2. Parameter sets for the propagation models of $\bar{p}$.

2.3 Anti-proton flux

The flux of $\bar{p}$ from the LSP decay is obtained by solving the diffusion equation:

$$\frac{\partial f_{\bar{p}}(E,\vec{x})}{\partial t} = K_{\bar{p}}(E)\nabla^2 f_{\bar{p}}(E,\vec{x}) - \frac{\partial}{\partial z}\left[V_c \mathrm{sign}(z) f_{\bar{p}}(E,\vec{x})\right] - 2h\delta(z)\Gamma_{\rm ann} f_{\bar{p}}(E,\vec{x}) + Q_{\bar{p}}(E,\vec{x}), \tag{2.13}$$

where z is the distance from the Galactic plane. Here, V_c is the convection velocity, h is the half height of the thin Galactic disc, which is taken to be $h = 100$ pc, and $\Gamma_{\rm ann}$ is the annihilation rate of $\bar{p}$ in the Galactic disc, which is given by

$$\Gamma_{\rm ann} = \left(n_{\rm H} + 4^{2/3} n_{\rm He}\right)\sigma_{p\bar{p}} v_{\bar{p}}, \tag{2.14}$$

where we use the number density of Hydrogen and Helium in the Galactic disc to be $n_{\rm H} = 1$ cm^{-3} and $n_{\rm He} = 0.07 n_{\rm H}$. The cross section $\sigma_{p\bar{p}}$ is given by [40, 41]

$$\sigma_{p\bar{p}} = \begin{cases} 661\left(1 + 0.0115 T_{\rm GeV}^{-0.774} - 0.948 T_{\rm GeV}^{0.0151}\right) \text{ mb} & : T_{\rm GeV} < 14.6 \text{ GeV} \\ 36 T_{\rm GeV}^{-0.5} \text{ mb} & : T_{\rm GeV} \geq 14.6 \text{ GeV} \end{cases}, \tag{2.15}$$

with $T_{\rm GeV}$ being the kinetic energy of the anti-proton in units of GeV. In addition, as in the case of $e^{\pm}$, the function $K_{\bar{p}}$ is parametrized as

$$K_{\bar{p}} = K_{\bar{p}}^{(0)} \beta_{\bar{p}} p_{\rm GeV}^{\delta}, \tag{2.16}$$

where $\beta_{\bar{p}}$ is the velocity of the anti-proton, and $p_{\rm GeV}$ is the momentum in units of GeV. Parameter sets for the diffusion equation used in our analysis are summarized in table 2. Again, the MED set gives the best-fit to the B/C analysis, while the maximal and minimal anti-proton fluxes are expected in the MAX and MIN sets. Once $f_{\bar{p}}$ is obtained, the anti-proton flux at the solar system is calculated as

$$\left[\Phi_{\bar{p}}(E)\right]_{\rm DM} = \frac{c\beta_{\bar{p}}}{4\pi} f_{\bar{p}}(E, \vec{x}_{\odot}). \tag{2.17}$$

2.4 γ-ray flux

The flux of the γ-ray is calculated by the sum of two contributions:

$$\left[\Phi_\gamma\right]_{\rm DM} = \left[\Phi_\gamma\right]_{\rm cosmo} + \left[\Phi_\gamma\right]_{\rm halo}, \tag{2.18}$$

JHEP05(2009)110

where the first and second terms in the right-hand side are fluxes of γ-ray from cosmological distance and that from the Milky Way halo, respectively.[4]

The flux from cosmological distance $[\Phi_\gamma]_{\rm cosmo}$ is obtained as

$$[\Phi_\gamma]_{\rm cosmo} = \frac{1}{m_{\rm LSP}\tau_{\rm LSP}} \int_E^\infty dE' G_\gamma(E, E') \left[\frac{dN_\gamma}{dE'}\right]_{\rm dec} . \tag{2.19}$$

Here, the propagation function of γ-ray turns out to be

$$G_\gamma(E, E') = \frac{c\rho_c \Omega_{\rm LSP}}{4\pi H_0 \Omega_M^{1/2}} \frac{1}{E} \left(\frac{E}{E'}\right)^{3/2} \frac{1}{\sqrt{1 + \Omega_\Lambda/\Omega_M (E/E')^3}}, \tag{2.20}$$

where H_0 is present Hubble expansion rate, ρ_c is critical density, while $\Omega_M \simeq 0.137\ h^{-2}$ and $\Omega_\Lambda \simeq 0.721$ (with $h \simeq 0.701$) are density parameters of total matter and dark energy, respectively [1]. On the other hand, the flux from the Milky Way halo $[\Phi_\gamma]_{\rm halo}$ is calculated as

$$[\Phi_\gamma]_{\rm halo} = \frac{1}{m_{\rm LSP}\tau_{\rm LSP}} \frac{1}{4\pi} \left[\frac{dN_\gamma}{dE'}\right]_{\rm dec} \left\langle \int_{\rm l.o.s.} \rho_{\rm DM}(\vec{l})\ d\vec{l} \right\rangle_{\rm dir} , \tag{2.21}$$

where the integration should be understood to extend over the line of sight (l.o.s.) and $\langle \cdots \rangle_{\rm dir}$ means averaging over the direction. In the EGRET observation [42], the signal from the Galactic disc is excluded in order to avoid the noise. Thus, in order to compare our numerical results with the EGRET observation, we exclude the region within $\pm 10^\circ$ around the Galactic disc in the averaging.

For the background flux against the signal, we adopt the following flux formula which is estimated from the EGRET observation in the energy range $0.05\ {\rm GeV} \leq E \leq 0.15\ {\rm GeV}$ [44]:

$$E^2\,[\Phi_\gamma]_{\rm BG} \simeq 5.18 \times 10^{-7}\ ({\rm cm}^2\ {\rm sec\ str})^{-1}\ {\rm GeV} \times \left(\frac{E}{\rm GeV}\right)^{-0.449} . \tag{2.22}$$

We have assumed that the spectrum of the background flux from astrophysical origins follows a power law, and its behavior can be extracted to the high energy region. The total γ-ray spectrum is then given by

$$[\Phi_\gamma]_{\rm tot} = [\Phi_\gamma]_{\rm DM} + [\Phi_\gamma]_{\rm BG} . \tag{2.23}$$

3 Gravitino LSP

Now, we are at the position to discuss the fluxes of $e^\pm$ for individual dark matter scenarios. The first example is the case where the gravitino, which is denoted as ψ_μ, is the LSP and

[4] γ-ray may be also produced by the inverse Compton (IC) scattering process. We have estimated the γ-ray flux from the IC process with the cosmic microwave background radiation in the sky region $10^\circ < b < 20^\circ$ (with b here being Galactic longitude) to compare with the preliminary FERMI results, and found that the flux is much smaller than the FERMI data. Detailed study of the γ-ray flux from the IC process will be given elsewhere [43].

JHEP05(2009)110

hence is dark matter. The model discussed here is the same as that given in [44–46], and we consider the following RPV interaction

$$\mathcal{L}_{\rm RPV} = B_i \tilde{L}_i H_u + m^2_{\tilde{L}_i H_d} \tilde{L}_i H_d^* + \text{h.c.}, \tag{3.1}$$

where $\tilde{L}_i$ is left-handed slepton doublet in i-th generation, while H_u and H_d are up- and down-type Higgs boson doublets, respectively. (In the present analysis, H_d and $\tilde{L}_i$ are defined in the frame in which the bi-linear R-parity violating terms in the superpotential vanish.)

The effects of the RPV with (3.1) is parametrized by the VEV of the sneutrino fields $\tilde{\nu}_i$. To parametrize the VEV of $\tilde{\nu}_i$, we define

$$\kappa_i \equiv \frac{\langle \tilde{\nu}_i \rangle}{v} = \frac{B_i \sin\beta + m^2_{\tilde{L}_i H_d} \cos\beta}{m^2_{\tilde{\nu}_i}}, \tag{3.2}$$

where $v \simeq 174$ GeV is the VEV of standard-model-like Higgs boson, $\tan\beta = \langle H_u^0 \rangle / \langle H_d^0 \rangle$, and $m_{\tilde{\nu}_i}$ is the mass of $\tilde{\nu}_i$. Since we are interested in the case of very long lifetime, we consider the case that $\kappa_i \ll 1$.

With the RPV operator given in eq. (3.1), the gravitino decays as $\psi_\mu \to \gamma\nu_i$, $Z\nu_i$, Wl_i, and $h\nu_i$. (For detailed calculations of the decay rates for these processes, see in [44].) In particular, in the limit that the gravitino is much heavier than the weak bosons, the following relation holds: $\Gamma_{\psi_\mu \to Z\nu_i} \simeq \Gamma_{\psi_\mu \to h\nu_i} \simeq \frac{1}{2}\Gamma_{\psi_\mu \to W l_i}$, and the process $\psi_\mu \to \gamma\nu_i$ is suppressed. Then, once the relic gravitino decays, the produced l_i (as well as the weak and Higgs bosons) becomes the source of cosmic-ray electron and positron. In addition, with the hadronic decay of the weak and Higgs bosons, energetic anti-proton and γ-ray are also produced. Fluxes of these particles have been measured, and in the following, we compare the expected fluxes with the results of observations.

As we have seen, the fluxes of the cosmic rays originating from the gravitino decay is inversely proportional to the lifetime of the gravitino $\tau_{3/2}$. With the RPV interaction given in eq. (3.1), the lifetime of the gravitino is approximately given by

$$\tau_{3/2} \simeq 6 \times 10^{25}\ \text{sec} \times \left(\frac{\kappa}{10^{-10}}\right)^{-2} \left(\frac{m_{3/2}}{1\ \text{TeV}}\right)^{-3}, \tag{3.3}$$

where

$$\kappa^2 \equiv \sum_i \kappa_i^2. \tag{3.4}$$

Now, we show the cosmic-ray fluxes originating from the gravitino decay. First, we consider the fluxes of $e^\pm$, motivated by their observed anomalous fluxes recently reported by the PAMELA and ATIC experiments. In order to discuss the preferred lifetime to explain the anomalous positron fraction observed by the PAMELA experiment, we define the χ^2 variable as

$$\chi^2 = \sum_i \frac{\left(R^{(\rm obs)}_{e^+,i} - R^{(\rm th)}_{e^+,i}\right)^2}{\delta R^{(\rm obs)2}_{e^+,i}}, \tag{3.5}$$

JHEP05(2009)110

where $R^{(\mathrm{obs})}_{e^+,i}$ and $R^{(\mathrm{th})}_{e^+,i}$ are positron fraction in i-th bin measured by the PAMELA and that predicted in the unstable dark matter scenario, respectively, and $\delta R^{(\mathrm{obs})}_{e^+,i}$ is the error in the observed fraction. Since the positron flux in the low-energy region is sensitive to the background fluxes, we only use the data points with $E \geq 15$ GeV (5 data points) in the calculation of χ^2. (As we will discuss, the positron fraction depends on the background. We use the χ^2 variable just to estimate the preferred value of the lifetime to explain the PAMELA results.)

The best-fit lifetime to explain the PAMELA anomaly depends on the gravitino mass, the flavor of the final-state lepton, and the propagation parameters. In our analysis, for simplicity, we consider the cases where the LSP dominantly decays into fermions in one of the three generations. Concerning the other parameters, we will discuss how the resultant fluxes depend on them.

For the case where the gravitino decays only into the first-generation lepton, we plot the positron fraction in figure 1 with the best-fit lifetime. Here, we show results with adopting the MED and M2 propagation models, because the results with the M1 and MED models are almost the same. For the MED (M2) propagation model, the best-fit lifetime is given by 2.0×10^{26} sec, 1.1×10^{26} sec, and 8.6×10^{25} sec (9.3×10^{25} sec, 5.0×10^{25} sec, and 4.3×10^{25} sec) for $m_{3/2} = 300$ GeV, 600 GeV, and 1.2 TeV, respectively.

The positron fraction for the cases where the gravitino decays only into second- and third-generation lepton are shown in figures 2 and 3, respectively. Here, we show the results with the propagation models MED and M2. We can see that the predicted positron fraction well agrees with the PAMELA result if the lifetime is properly chosen. In particular, when the final-state lepton is first- (second-) generation, the fit is excellent irrespective of the gravitino mass with MED (M2) propagation model. We note here that, for e^-, the background flux is significantly larger than the signal flux, while the dark matter contribution dominates for e^+. Thus, the result is sensitive to the choice of background because we plot the positron fraction. However, the theoretical calculation of the positron fraction contains parameters both in the particle-physics model (i.e., the lifetime and the flavor of the final-state leptons) and in the propagation model. Thus, we believe that positron fraction observed by the PAMELA can be explained in the present scenario with other choice of the background fluxes. For example, even if the normalization of the background e^- flux is changed, we can obtain almost the same positron fraction by varying the lifetime.

Next, we consider the total flux $\Phi_{e^+} + \Phi_{e^-}$. The numerical results are shown in figures 4–6 for the cases where the gravitino decays only into first-, second-, or third-generation lepton. For the calculation of $\Phi_{e^+} + \Phi_{e^-}$, we use the best-fit lifetime to fit the PAMELA data. In the figures, it can be seen that the observed anomalous structure is well reproduced with both MED and M2 models by relevantly choosing $m_{3/2}$, except for the case that final-state lepton is third-generation. For the case of final-state lepton being in the first- (second-) generation, the result is a good agreement with the observation when $m_{3/2} \simeq 1.2\,\mathrm{TeV}$ (2 TeV). Here, we note that the total flux is not sensitive to the background because the signal from the dark matter is larger than (or at least comparable to) the background.

JHEP05(2009)110

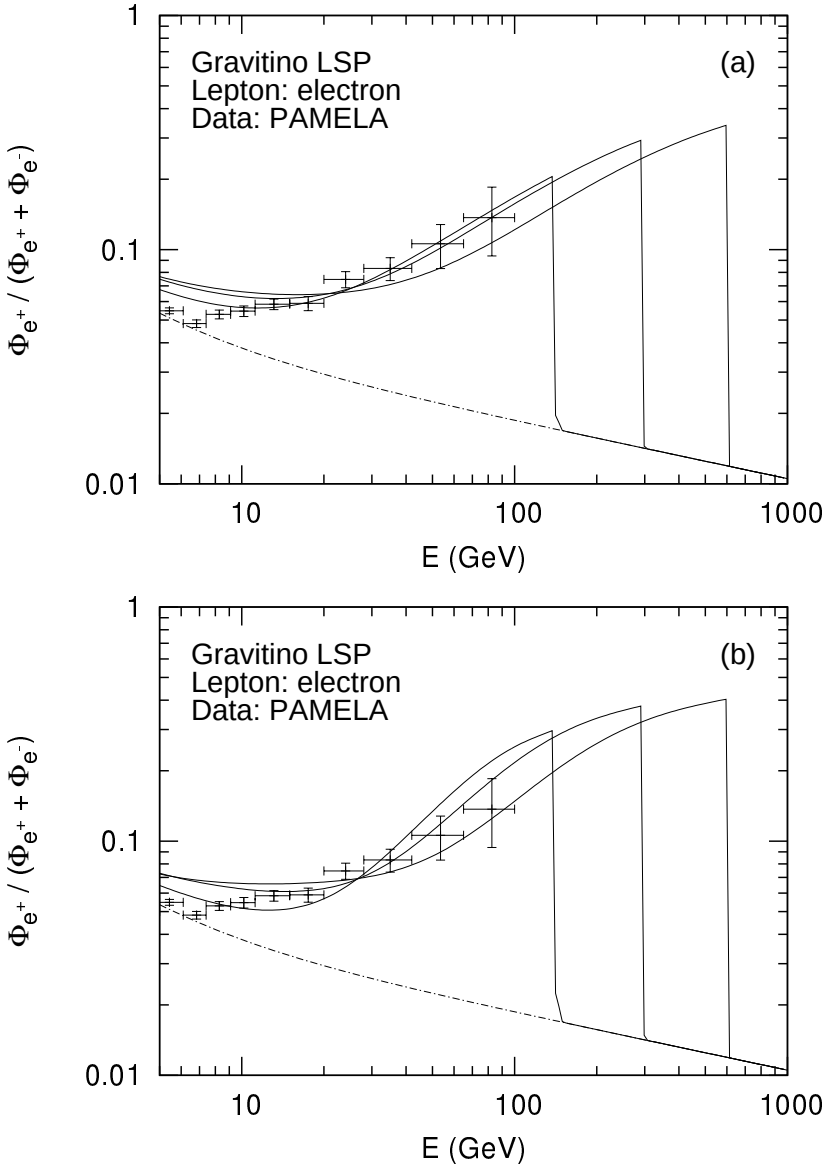

Figure 1. Positron fractions in (a) MED and (b) M2 models for the case where the gravitino dominantly decays to the first-generation lepton. Dot-dashed line is the positron fraction calculated only by the background fluxes. Here, we take $m_{3/2} = 300$ GeV, 600 GeV, and 1.2 TeV (from left to right) with 2.0 $\times 10^{26}$ sec, 1.1 $\times 10^{26}$ sec, and 8.6 $\times 10^{25}$ sec (9.3 $\times 10^{25}$ sec, 5.0 $\times 10^{25}$ sec, and 4.3 $\times 10^{25}$ sec) in MED (M2) model, respectively.

With the decay of the gravitino dark matter, energetic γ-ray and anti-proton are also produced. Thus, with the observations of the fluxes of these particles, we may confirm or exclude the present scenario.[5] Notice that γ and $\bar{p}$ are mostly from the hadronic decays of

[5]High energy γ-ray from the Galactic center has been calculated in the scenario where dark matter annihilates into W^+W^- pair [18, 48]. We have checked that the high energy γ-ray flux in the present

JHEP05(2009)110

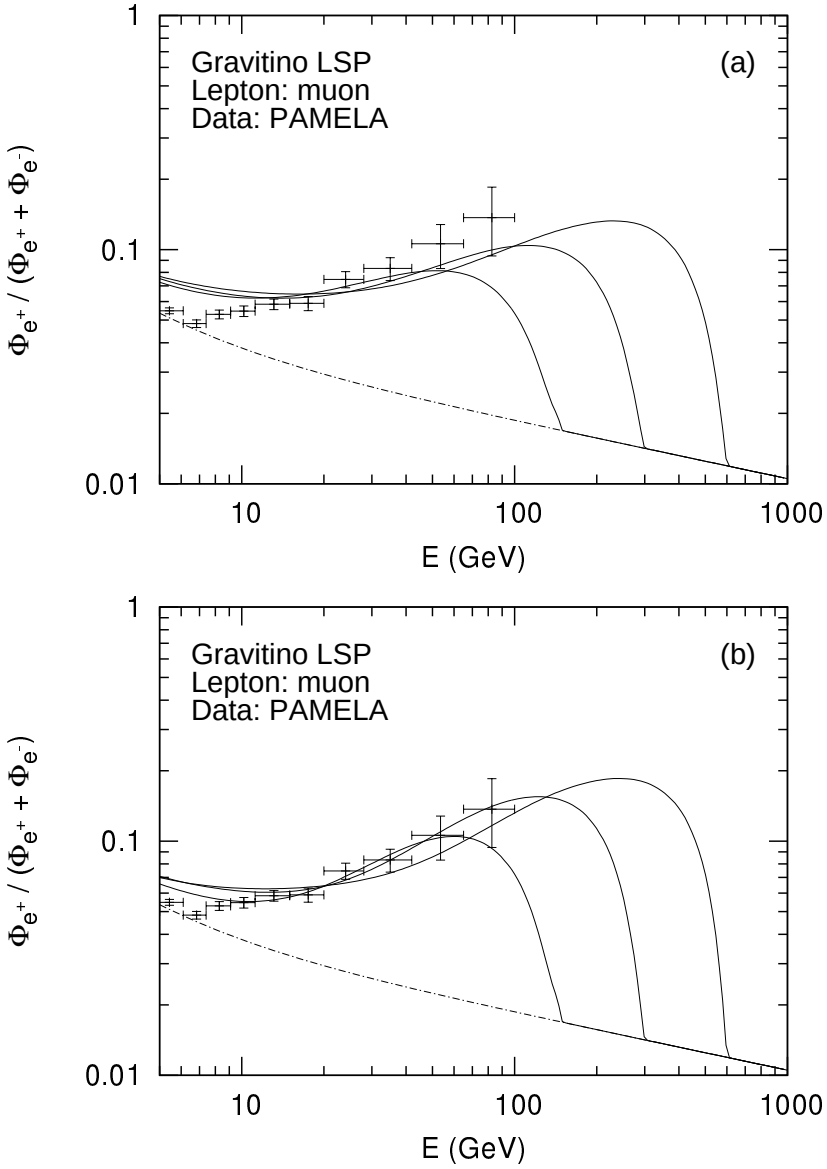

Figure 2. Same as figure 1, but for the case where the gravitino dominantly decays to second-generation lepton. Here, we take $\tau_{3/2} = 1.5\times10^{26}$ sec, 1.1×10^{26} sec, and 8.6×10^{25} sec (9.3×10^{26} sec, 5.8×10^{26} sec, and 5.0×10^{25} sec) in MED (M2) model, which are the best-fit lifetime.

the weak and Higgs bosons. Thus, the fluxes of these particles are insensitive to the flavor of the final-state lepton, except for the case where τ-lepton is produced by the decay. (See the following discussion.)

In figure 7, we plot the flux of the γ-ray in the present scenario with the primary

scenario is much smaller than that in the annihilating scenario (into W^+W^- pair), assuming that the PAMELA and ATIC anomalies are from the decay or the annihilation of dark matter. Then, we found that the total γ-ray flux in the present scenario is consistent with the HESS observation [49].

JHEP05(2009)110

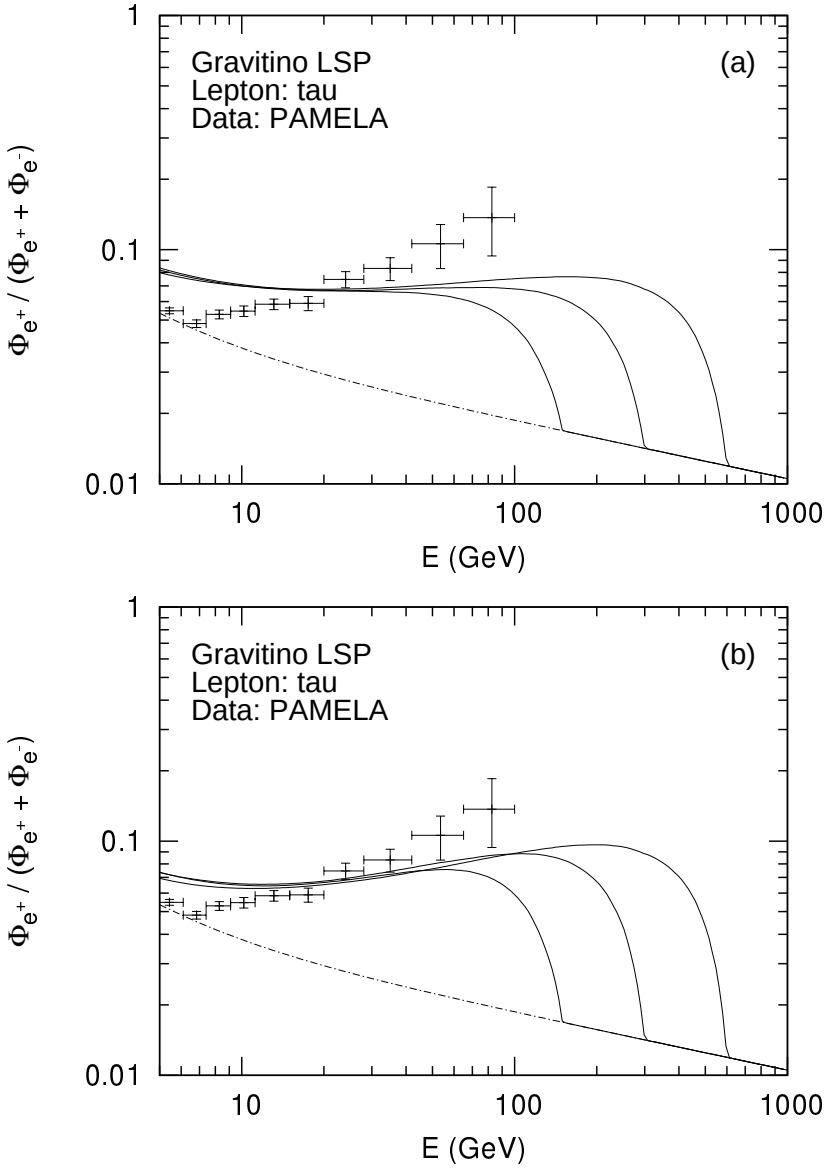

Figure 3. Same as figure 15, but for the case where the gravitino dominantly decays to third-generation lepton. Here, we take $\tau_{3/2} = 9.3\times10^{25}$ sec, 8.6×10^{25} sec, and 7.9×10^{25} sec (6.3×10^{25} sec, 5.4×10^{25} sec, and 5.4×10^{25} sec) in MED (M2) model, which are the best-fit lifetime.

lepton being in first- or second-generation. From the figure, we see that the expected γ-ray flux well agrees with EGRET data irrespective of $m_{3/2}$. Because the flux from the gravitino decay is larger than the background, the γ-ray flux does not highly depend on the background.[6] On the other hand, if the primary lepton produced in the decay is in

[6]The recent preliminary results of the FERMI satellite (for the region $10^\circ < b < 20^\circ$) indicates no anomalous excess in the high energy γ-ray [50]. We have also calculated the γ-ray flux for the region $10^\circ < b < 20^\circ$ in the present scenario, and found that the dark-matter contribution to the flux for such a

JHEP05(2009)110

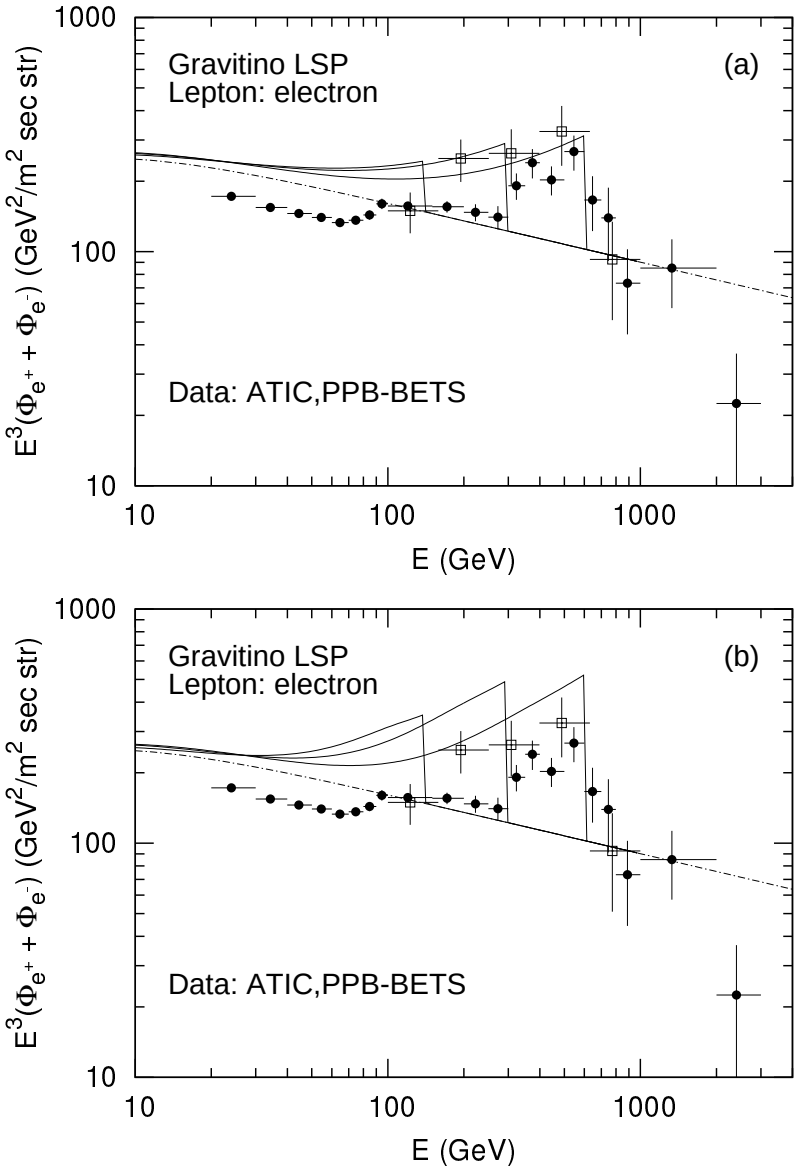

Figure 4. Total fluxes of positron and electron in (a) MED and (b) M2 models for the case where the gravitino dominantly decays to the first-generation lepton. Dot-dashed line is the background flux. Here, we take the the same mass and lifetime as figure 1, and also plot PPB-BETS data [47].

third-genaration, γ from π^0 decay also contributes to the total flux [51]. In figure 8, we show the result for such a case. From the figure, one can see an increase of the flux in the high energy region of $E \gtrsim 100\,\mathrm{GeV}$.

The anti-proton flux from the decay of the gravitino dark matter is shown in figures 9–11. We can see that the anti-proton flux depends on the propagation model. However, with the MED and MIN models, the flux from the gravitino decay is comparable to

region is smaller than the FERMI data.

JHEP05(2009)110

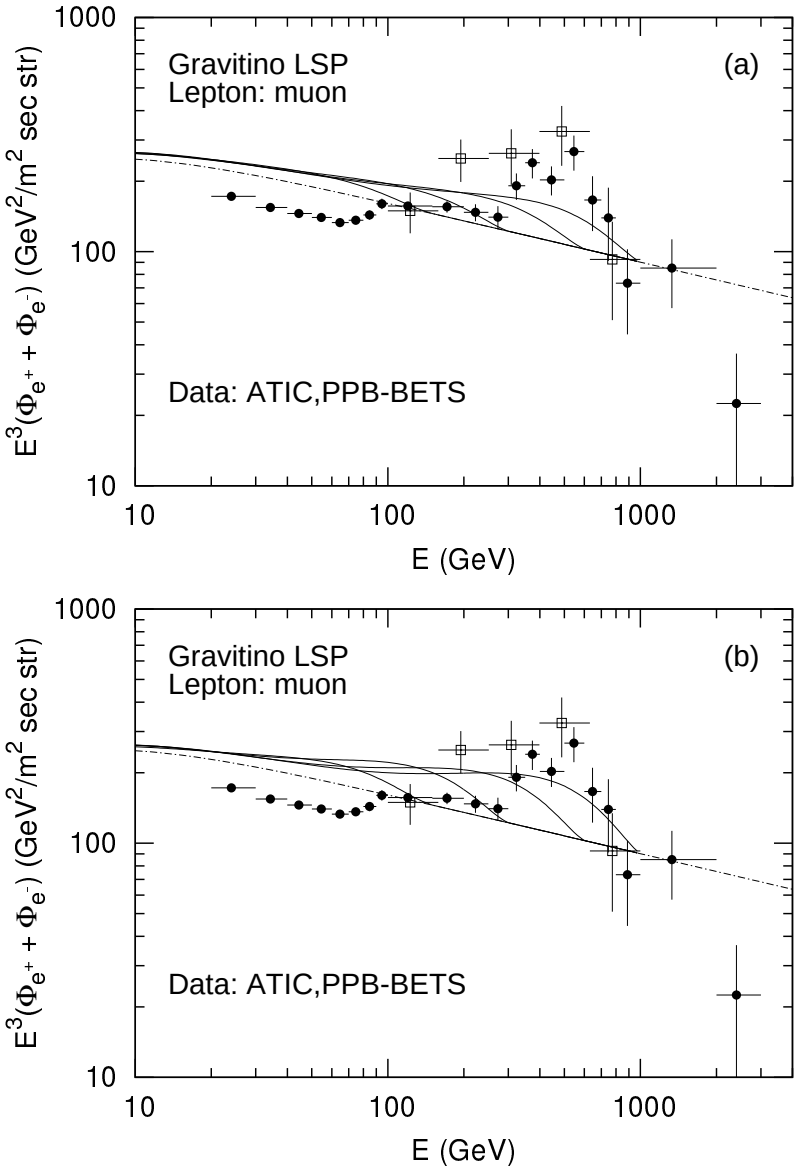

Figure 5. Same as figure 4, but the gravitino dominantly decays to second-generation lepton. We take the the same mass and lifetime as figure 2, and also take $m_{3/2} = 2$ TeV with $\tau_{3/2} = 7.4 \times 10^{25}$ sec and 4.6×10^{25} sec in (a) and (b), respectively.

or smaller than the observed fluxes.[7] Thus, we conclude that the present scenario is not excluded by the observation of the cosmic-ray $\bar{p}$ flux, taking account of the uncertainties in the propagation model and estimation of the background. However, if a better understand-

[7]We also estimated anti-proton to proton ratio to compare recent data by PAMELA [52], using the proton flux observed by BESS [53] and CAPRICE [54]. Then we found that the $\bar{p}/p$ ratio is order of magnitude smaller than the PAMELA data if we take the MIN propagation model and that it is comparable to or a few times larger than the PAMELA data with MED model. Thus, taking account account of the uncertainties in the propagation model as well as those in the background proton flux, the present scenario is not excluded yet.

JHEP05(2009)110

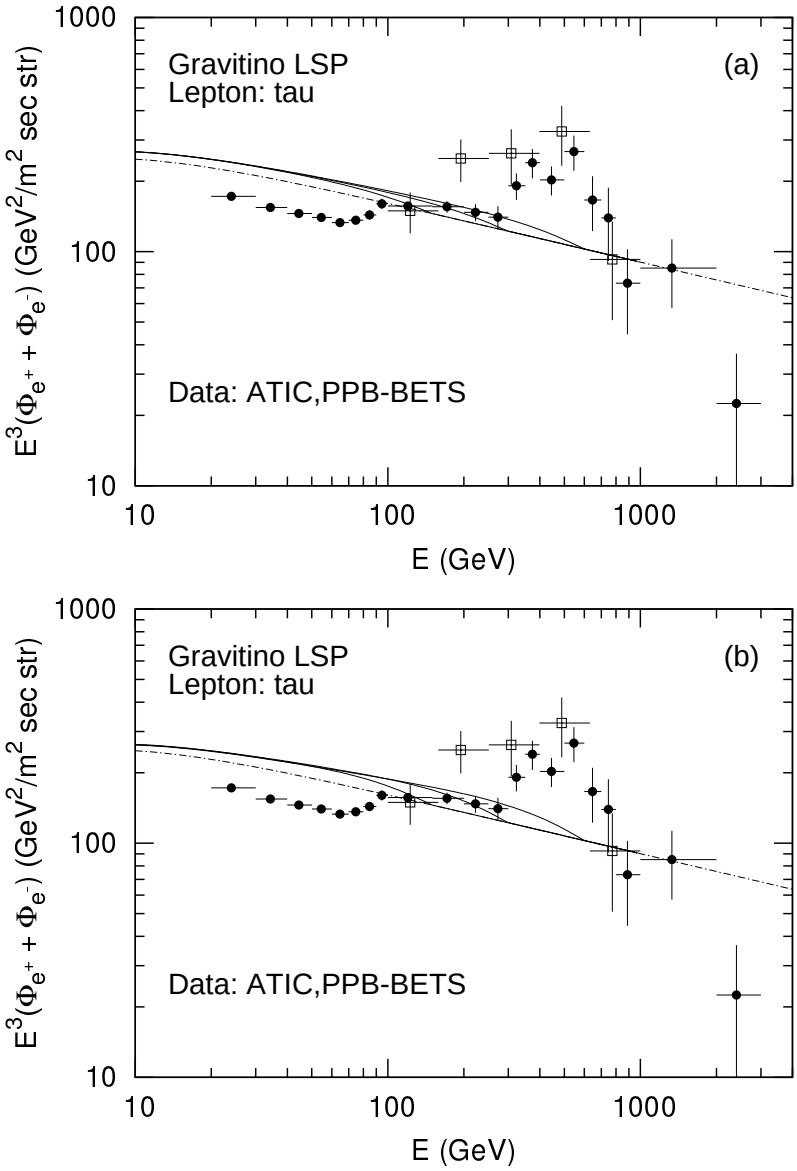

Figure 6. Same as figure 4, but the gravitino dominantly decays to third-generation lepton. We take the the same mass and lifetime as figure 3.

ing of the propagation of the anti-proton becomes available in the future, it will provide a significant test of the present scenario.

Before closing this section, we comment that this scenario may be tested by the LHC experiment. Indeed, in this scenario, the lightest superparticle in the MSSM sector (which we call MSSM-LSP) may decay inside the detector. In the present scenario, the MSSM-LSP is likely to decay to the standard model particles via the RPV interaction even though there exists a superparticle (i.e., gravitino) lighter than the MSSM-LSP. As we have mentioned, the κ parameter is expected to be $O(10^{-10})$, which gives the lifetime of the MSSM-LSP of the order of $\sim 10^{-(4-5)}$ sec. Thus, the typical decay length of the MSSM-LSP is expected

JHEP05(2009)110

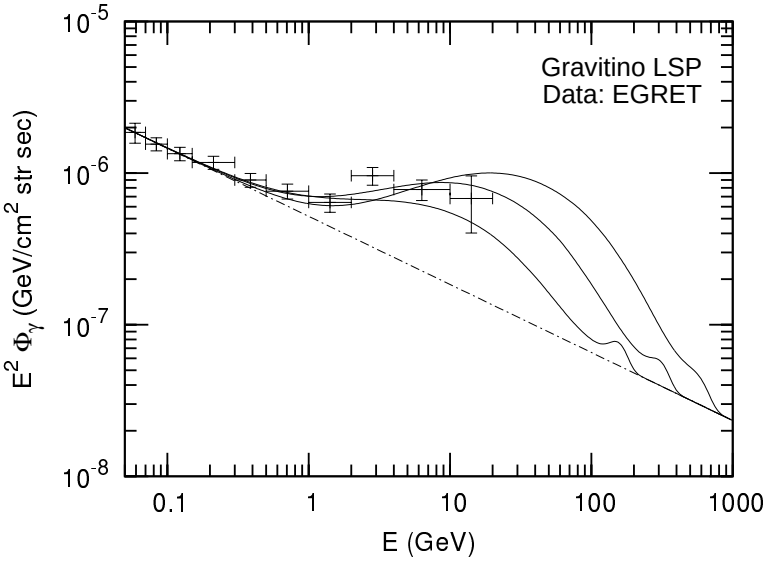

Figure 7. γ-ray flux. Dot-dashed line is the background flux. Here, we take mass and lifetime as the same as figure (a) in figure 1

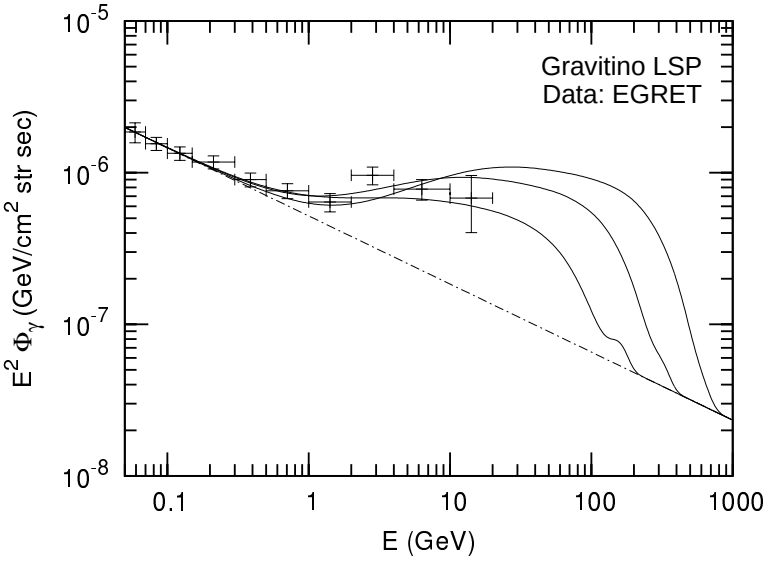

Figure 8. The same as figure 7, but for the case where primary lepton produced in the decay is third-genaration.

to be much longer than the sizes of the ATLAS and CMS detectors. However, since enormous amount of SUSY events is expected at the LHC experiment, some of the MSSM-LSP produced at the LHC may decay inside the detector, which results in drastic signal, like a displaced vertex or a kink in a high-energy charged track. In addition, if such decay processes can be observed, it may be also possible to constrain the lifetime of the MSSM-LSP, which may be used for the determination of the κ parameter [57].

JHEP05(2009)110

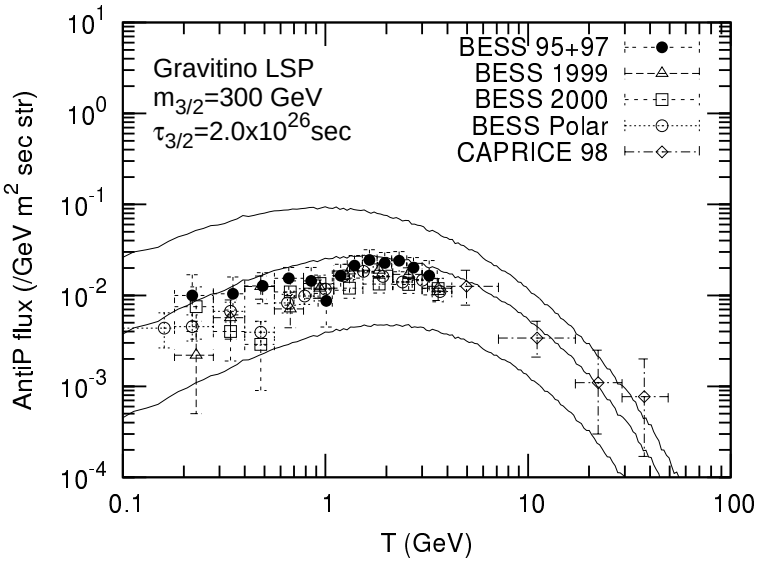

Figure 9. Anti-proton flux in MIN, MED, and MAX models. Here, we take $m_{3/2} = 300$ GeV and $\tau_{3/2} = 2.0 \times 10^{26}$ sec, which is the best-fit lifetime in the case that the gravitino dominantly decays to first-generation lepton, and also plot the observation data by BESS [55] and CAPRICE [56].

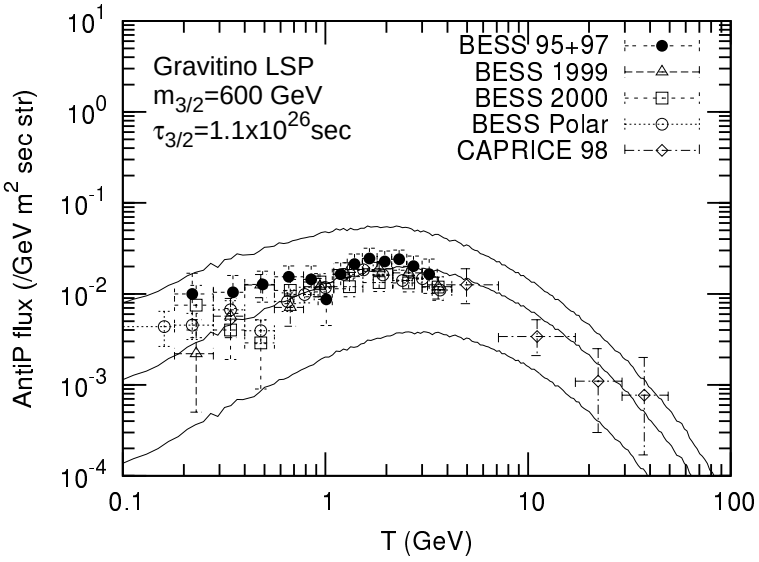

Figure 10. Same as figure 9, except for taking $m_{3/2} = 600\,\text{GeV}$ and corresponding best-fit lifetime.

4 Neutralino LSP

In the previous section, we have considered the case that the gravitino is the LSP. In conventional SUSY models, another important candidate for the LSP is the lightest neutralino, which is a linear combination of Bino, neutral Wino, and two neutral Higgsinos. To make our discussion simple, in this section, we assume that the lightest neutralino is (almost) Bino-like. This is the case, for example, in large fraction of the parameter space of models

JHEP05(2009)110

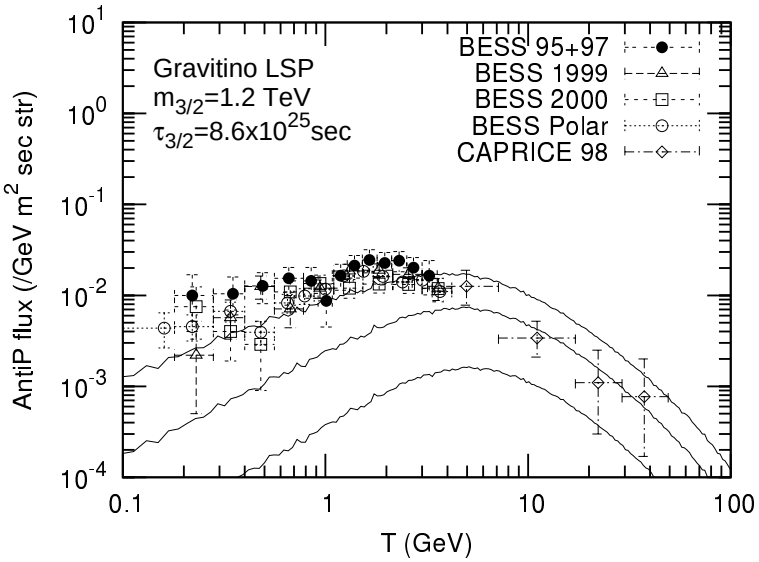

Figure 11. Same as figure 9, except for taking $m_{3/2} = 1.2\,\text{TeV}$ and corresponding best-fit lifetime.

with the grand-unification condition among gaugino masses.

With the RPV operators given in eq. (3.1), the Bino-like neutralino $\tilde{B}$ decays as $\tilde{B} \to Z\nu_i$, Wl_i, and $h\nu_i$. Decay rates for these processes are given by[8]

$$\Gamma_{\tilde{B}\to Z\nu_i} = \frac{1}{128\pi} g_Z^2 \sin^2\theta_W \kappa_i^2 \; m_{\tilde{B}} \left(1 - 3\frac{m_Z^4}{m_{\tilde{B}}^4} + 2\frac{m_Z^6}{m_{\tilde{B}}^6}\right), \tag{4.1}$$

$$\Gamma_{\tilde{B}\to Wl_i} = \frac{1}{64\pi} g_Z^2 \sin^2\theta_W \kappa_i^2 \; m_{\tilde{B}} \left(1 - 3\frac{m_W^4}{m_{\tilde{B}}^4} + 2\frac{m_W^6}{m_{\tilde{B}}^6}\right), \tag{4.2}$$

$$\Gamma_{\tilde{B}\to h\nu_i} = \frac{1}{128\pi} g_Z^2 \sin^2\theta_W \kappa_i^2 \; m_{\tilde{B}} \left(\frac{m_{\tilde{\nu}}^2}{m_{\tilde{\nu}}^2 - m_h^2}\right)^2 \left(1 - \frac{m_h^2}{m_{\tilde{B}}^2}\right)^2, \tag{4.3}$$

where $g_Z = \sqrt{g_1^2 + g_2^2}$ (with g_1 and g_2 being the gauge coupling constants of the $\text{U}(1)_Y$ and $\text{SU}(2)_L$ gauge groups, respectively), θ_W is the Weinberg angle, $m_{\tilde{B}}$ is Bino-like neutralino mass, and m_Z, m_W, m_h are masses of corresponding gauge and Higgs bosons.

As one can see from the above decay rates, we obtain the relation $\Gamma_{\tilde{B}\to Z\nu_i} \simeq \Gamma_{\tilde{B}\to h\nu_i} \simeq \frac{1}{2}\Gamma_{\tilde{B}\to Wl_i}$. Remember that, for the case of the gravitino LSP, the same (approximated) relation holds. Thus, the fluxes of the high energy cosmic rays in the Bino LSP case is expected to be similar to that in the gravitino LSP case as far as the lifetime is $\sim 10^{26}$ sec. Since the decay rate of the Bino is not suppressed by the Planck scale, the size of the κ_i parameter relevant to explain the PAMELA and ATIC anomalies is much smaller than that in the gravitino LSP case. Indeed, with the decay rates given in eq. (4.1) – (4.3), the lifetime of the Bino LSP in the present case is estimated as

$$\tau_{\tilde{B}} \simeq 2 \times 10^{25}\ \text{sec} \times \left(\frac{\kappa}{10^{-25}}\right)^{-2} \left(\frac{m_{\tilde{B}}}{1\ \text{TeV}}\right)^{-1}. \tag{4.4}$$

[8]Here, we assume that the lightest Higgs boson is almost standard-model like.

JHEP05(2009)110

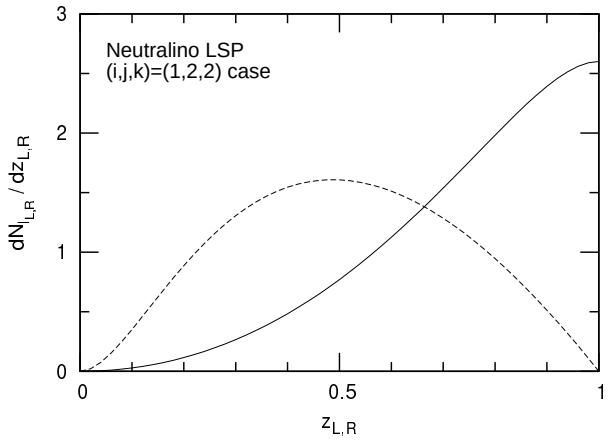

Figure 12. Distribution of the left- (solid) and right-handed (dashed) charged leptons emitted from the Bino decay via the $\hat{L}\hat{L}\hat{E}^c$-type superpotential. Here, we take $m_{\tilde{l}_R}/m_{\tilde{B}} = 1.2$.

So far, we have considered the bi-linear RPV interaction given in eq. (3.1). In such a case, as we have discussed, high energy γ and anti-proton are also produced by the decay of the LSP. However, if we consider other types of RPV interactions, it may be possible to enhance the e^+ and e^- fluxes without affecting γ-ray and anti-proton fluxes. This is the case where the Bino LSP decays mainly via the PRV superpotential:

$$W_{\rm RPV} = \frac{1}{2}\lambda_{ijk}\hat{L}_i\hat{L}_j\hat{E}^c_k, \tag{4.5}$$

where $\lambda_{ijk} = -\lambda_{jik}$. With this superpotential, the Bino decays as $\tilde{B} \to \nu_i l^\pm_{L,j} l^\mp_{R,k}$ and $\nu_j l^\pm_{L,i} l^\mp_{R,k}$ via diagrams with a (virtual) slepton propagation. Hereafter, let us consider the e^+ and e^- fluxes in such a case.

With the above superpotential, the Bino decays into the three-body final state, and hence the final-state leptons are not monochromatic. For simplicity, we consider the case that the right-handed sleptons are lighter than left-handed ones, so that the diagram with the propagator of the right-handed slepton dominantly contributes to the Bino decay. Then, denoting the energies of $l^\pm_{L,j}$ and $l^\mp_{R,k}$ in the rest frame of $\tilde{B}$ as E_{l_L} and E_{l_R}, respectively, the energy distribution of the charged leptons for the process $\tilde{B} \to \nu_i l^\pm_{L,j} l^\mp_{R,k}$ is given by

$$\frac{d\Gamma_{\tilde{B}\to\nu_i l^\pm_{L,j} l^\mp_{R,k}}}{dE_{l_L} dE_{l_R}} = \frac{g_1 2\lambda_{ijk}2}{64\pi 3 m_{\tilde{B}}} \frac{z_{l_R}(1-z_{l_R})}{[(m_{\tilde{l}_{R,k}}/m_{\tilde{B}})2 - 1 + z_{l_R}]2}, \tag{4.6}$$

where $z_{l_{L,R}} \equiv 2E_{l_{L,R}}/m_{\tilde{B}}$. (Notice that $0 \le z_{l_{L,R}} \le 1$.)

In figure 12, we plot the energy distributions of the final-state leptons:

$$\frac{dN_{l_{L,R}}}{dz_{L,R}} \equiv \frac{1}{\Gamma_{\tilde{B}\to\nu_i l^\pm_{L,j} l^\mp_{R,k}}} \int dz_{l_{R,L}} \frac{d\Gamma_{\tilde{B}\to\nu_i l^\pm_{L,j} l^\mp_{R,k}}}{dz_{l_L} dz_{l_R}}. \tag{4.7}$$

Notice that this quantity depends only on the ratio $m_{\tilde{l}_{R,k}}/m_{\tilde{B}}$. (In the figure, we take $m_{\tilde{l}_R}/m_{\tilde{B}} = 1.2$.) As one can see, the left-handed lepton emitted in the decay is likely to be

JHEP05(2009)110

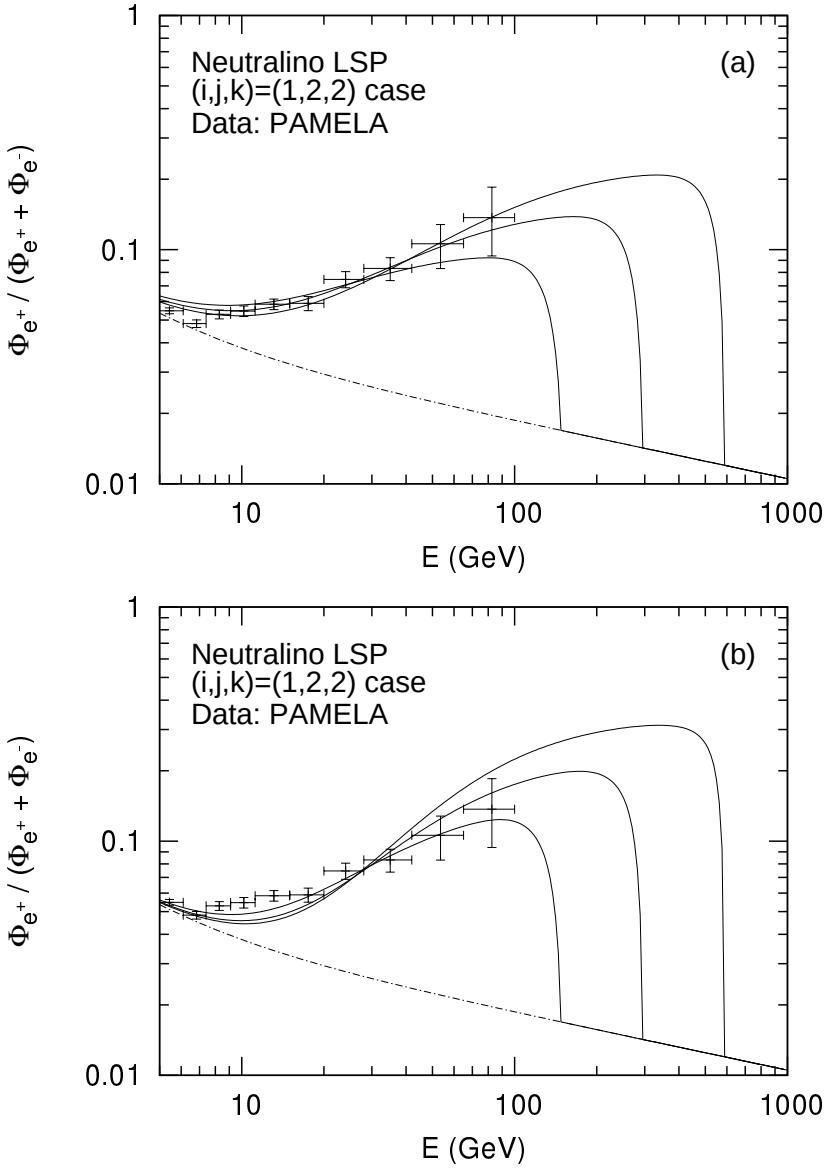

Figure 13. Positron fractions in (a) MED and (b) M2 models for the case where only λ_{122} is non-zero. Here, we take $m_{\tilde{B}} = 300$ GeV, 600 GeV, and 1.2 TeV from left to right and $\tau_{\tilde{B}} = 3.2 \times 10^{26}$ sec, 2.0×10^{26} sec, and 1.2×10^{26} sec (2.0×10^{26} sec, 1.1×10^{26} sec, and 5.0×10^{25} sec) in MED (M2) model, respectively.

energetic. Thus, if the coupling constant λ_{1jk} is sizable so that the Bino decays dominantly as $\tilde{B} \to e_L^{\pm} \nu_j l_{R,k}^{\mp}$, significant effects on the electron and positron fluxes are expected.

In figure 13, we show the positron fraction in the Bino dark matter case with the RPV superpotential given in eq. (4.5). Here, we consider the case that λ_{122} is the largest so that the Bino decays via this coupling, and we use $m_{\tilde{l}_R}/m_{\tilde{B}} = 1.2$. The best-fit lifetime to explain the PAMELA anomaly depends on $m_{\tilde{B}}$ as well as on the propagation model as in the

JHEP05(2009)110

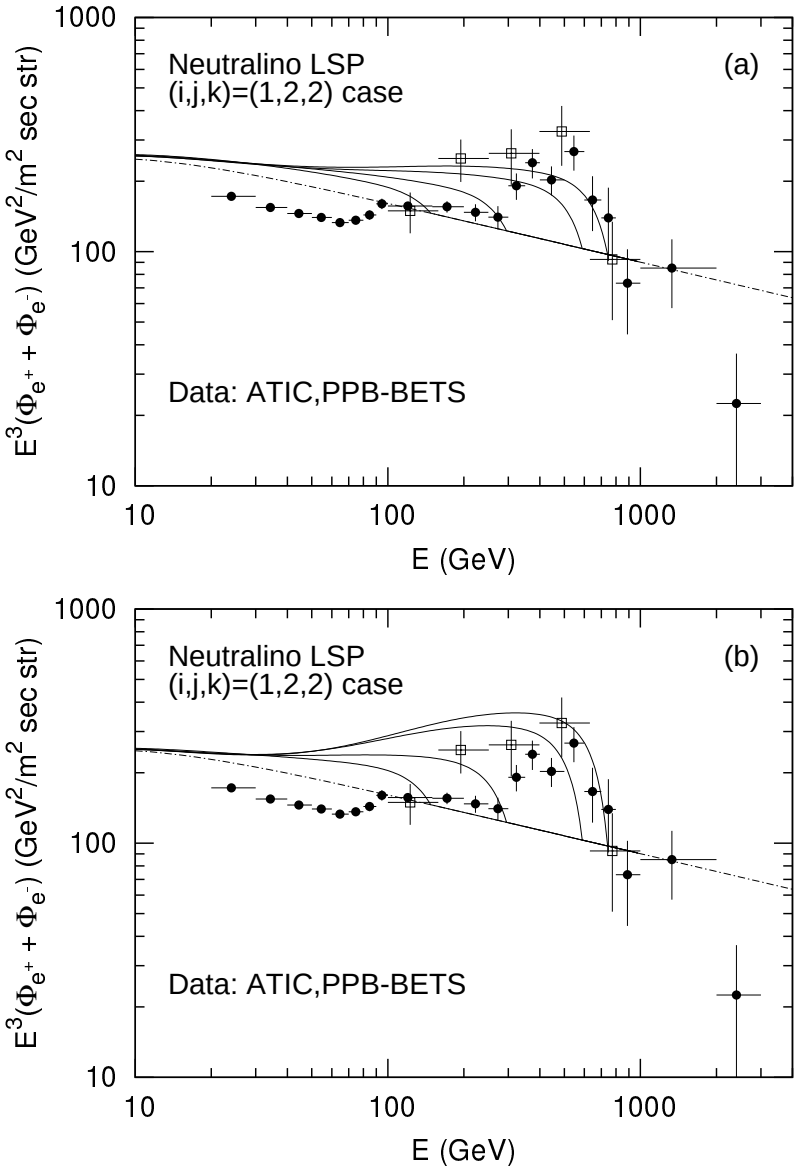

Figure 14. Total fluxes in (a) MED and (b) M2 models for the case where only λ_{122} is non-zero. We take the same values for $m_{\tilde{B}}$ and $\tau_{\tilde{B}}$ in figure 13, and also take $m_{\tilde{B}} = 1.5\,\mathrm{TeV}$ with $\tau_{\tilde{B}} = 9.3 \times 10^{25}$ sec (4.0×10^{25} sec) in (a)((b)).

case of the gravitino LSP. For the MED (M2) model of propagation, the best-fit lifetime is given by $\tau_{3/2} = 3.2 \times 10^{26}$ sec, 2.0×10^{26} sec, and 1.2×10^{25} sec (2.0×10^{26} sec, 1.1×10^{26} sec, and 5.0×10^{25} sec) for $m_{\tilde{B}} = 300$ GeV, 600 GeV, and 1.2 TeV, respectively. In addition, in figure 14, we plot the flux of $e^+ + e^-$. We can see that the simultaneous explanation of the PAMELA and ATIC/PPB-BETS anomalies may be possible in the present scenario if $m_{\tilde{B}} \simeq 1.5$ TeV and $\tau_{\tilde{B}} \simeq 9.3 \times 10^{25}$sec ($4.0 \times 10^{25}$ sec) for MED (M2) model.

So far, we have considered the case that λ_{122} is the largest. We have checked that

JHEP05(2009)110

similar results for the positron fraction and the total flux are obtained as far as the first-generation lepton is emitted in the decay. If $\tilde{B}$ decays only into second- and third-generation leptons, on the contrary, the total flux $\Phi_{e^+} + \Phi_{e^-}$ is suppressed compared to the observed values when we adopt the best-fit lifetime to explain the PAMELA anomaly.

5 Sneutrino LSP

The third candidate for the LSP is the sneutrino. In the framework of the MSSM, the sneutrino may not be a popular candidate for the LSP. However, the lightest sneutrino can be dark matter without conflicting phenomenological constraints, as we discuss below. In the previous section, we have seen that, with the $\hat{L}\hat{L}\hat{E}^c$ type RPV superpotential given in eq. (4.5), enhancement of electron and positron fluxes is possible without affecting the γ-ray and anti-proton fluxes. If the Bino is the LSP, the final-state leptons are not monochromatic, so that the end-point behavior of the cosmic-ray $e^{\pm}$ is smoothed. On the other hand, if the sneutrino is the LSP and hence is dark matter, and also if it decays via the $\hat{L}\hat{L}\hat{E}^c$ type RPV superpotential, shape of the $e^{\pm}$ spectrum drastically changes and a sharp edge at the end-point can be obtained [7].

In the MSSM, there only exist three left-handed sneutrinos $\tilde{\nu}_L$s ("L" means left-handed in this section), and one of them may be the lightest superparticle. By tuning the soft SUSY-breaking scalar and gaugino masses, the sneutrino becomes the LSP in some parameter region. In addition, the direct detection constraint on the sneutrino dark matter [58] can be avoided by introducing small lepton-number violating operator $\sim (\tilde{L}H_u)^2$ [59]. In addition, there is another possibility to realize the sneutrino dark matter scenario, in which the right-handed sneutrino $\tilde{\nu}_R$ becomes the LSP [60]. Since various neutrino-oscillation experiments suggest that the neutrinos are massive, we expect the existence of the right-handed (s)neutrinos. If the neutrino masses are Dirac-type, $\tilde{\nu}_R$ becomes as light as other MSSM superparticles in the gravity-mediation SUSY breaking scenario. (In other cases, $\tilde{\nu}_R$ may be much lighter than MSSM superparticles.) Thus, in some parameter space, $\tilde{\nu}_R$ can be the LSP. In such a case, $\tilde{\nu}_R$ can also be dark matter. The following arguments holds if $\tilde{\nu}_L$ or $\tilde{\nu}_R$ is the LSP.

If the sneutrino in i-th generation is the LSP, it decays as $\tilde{\nu}_i \to l_j^+ l_k^-$ assuming that the dominant RPV interaction is given by the $\hat{L}\hat{L}\hat{E}^c$ type RPV superpotential given in eq. (4.5). The decay rate of this process is

$$\Gamma_{\tilde{\nu}_i \to l_j^+ l_k^-} = \frac{\lambda_{ijk}^2 \theta_{\tilde{\nu}}^2}{16\pi} m_{\tilde{\nu}_i}, \tag{5.1}$$

where $\theta_{\tilde{\nu}}$ is the mixing parameter in the sneutrino sector. When the $\tilde{\nu}_L$ is the LSP, $\theta_{\tilde{\nu}} = 1$. Even if $\tilde{\nu}_i$ is right-handed, it decays via the RPV interaction given in eq. (4.5) because there should exist left-right mixing term of the sneutrinos, which is of the form

$$\mathcal{L}_{LR} = \delta m^2_{\tilde{\nu}_L \tilde{\nu}_R} \tilde{\nu}_L \tilde{\nu}_R + \text{h.c.} \tag{5.2}$$

In such a case, $\theta_{\tilde{\nu}}$ in eq. (5.1) should be

$$\theta_{\tilde{\nu}} = \frac{\delta m^2_{\tilde{\nu}_L \tilde{\nu}_R}}{m^2_{\tilde{\nu}_L} - m^2_{\tilde{\nu}_R}}. \tag{5.3}$$

JHEP05(2009)110

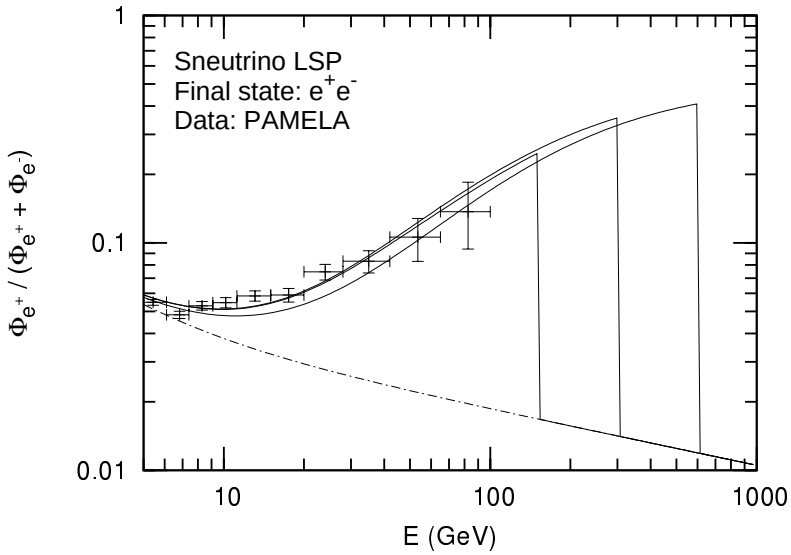

Figure 15. Positron fractions in MED model for the case where the sneutrino decays to the final state: e^+e^-. Here, we take $m_{\tilde{\nu}} = 300$ GeV, 600 GeV, and 1.2 TeV from left to right and $\tau_{\tilde{\nu}} = 5.4 \times 10^{26}$ sec, 2.5×10^{26} sec, and 1.6×10^{26} section

Thus, in any case, the sneutrino LSP decays into charged-lepton pair via the RPV interaction given in eq. (4.5). Thus, if the sneutrino is dark matter, those leptons become the source of cosmic-ray $e^{\pm}$. Importantly, in such a case, dark matter decays only leptonically, and the productions of hadrons and photon are irrelevant. Thus, the present model may produce significant amount of $e^{\pm}$ in cosmic ray without affecting the anti-proton and γ-ray fluxes.

In the following, we calculate the electron and positron fluxes from the decay of sneutrino dark matter. Here, we take $m_{\tilde{\nu}} = 300$ GeV, 600 GeV, and 1.2 TeV. The resultant flux depends on the flavors of the final-state leptons. Here, for simplicity, we consider three simple decay modes: $\tilde{\nu} \to e^+e^-$, $\mu^+\mu^-$, and $\tau^+\tau^-$.

The results of the calculations of positron fraction are shown in figure 15 − 17, where MED mode of the propagation is adopted. In addition, we use the best-fit lifetime for each $m_{\tilde{\nu}}$. We see good agreements with the observation for all the cases. We have also checked that a reasonable agreement between the prediction and the PAMELA data is obtained even with the M2 model if the sneutrino decays into $\mu^+\mu^-$ and $\tau^+\tau^-$.

Next, we discuss the total flux $\Phi_{e^+} + \Phi_{e^-}$. The numerical results are shown in figures 18–20, taking the same parameters as in figure 15–17, respectively. One can see the anomalous behavior is explained when $m_{\tilde{\nu}} \sim 1.2 - 1.5$ TeV in the cases of final state: e^+e^- and $\mu^+\mu^-$ with MED model. In addition, we checked that the same anomalous behavior is obtained in the case of final state: $\mu^+\mu^-$ with M2 model.

JHEP05(2009)110

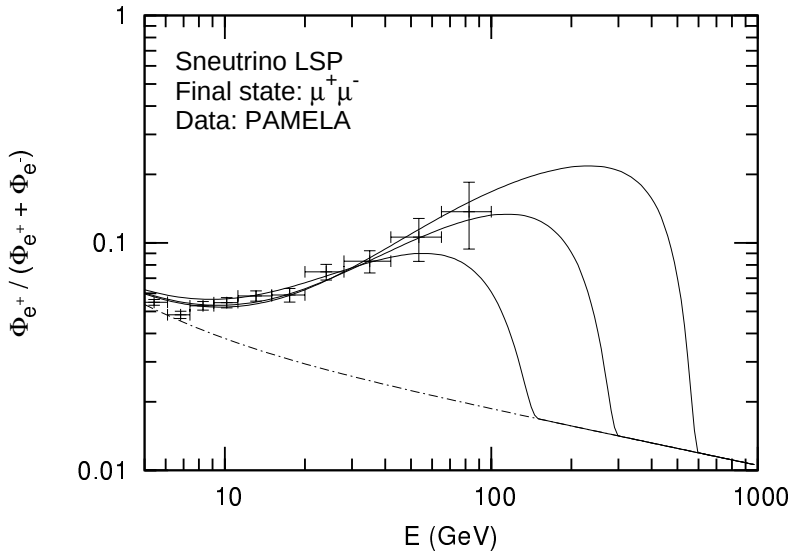

Figure 16. Same as figure 15 in the case of final state: $\mu^+\mu^-$. Here, we take $\tau_{\tilde{\nu}} = 3.7 \times 10^{26}$ sec, 2.3×10^{26} sec, and 1.2×10^{26} sec, which are the best-fit lifetime with MED model.

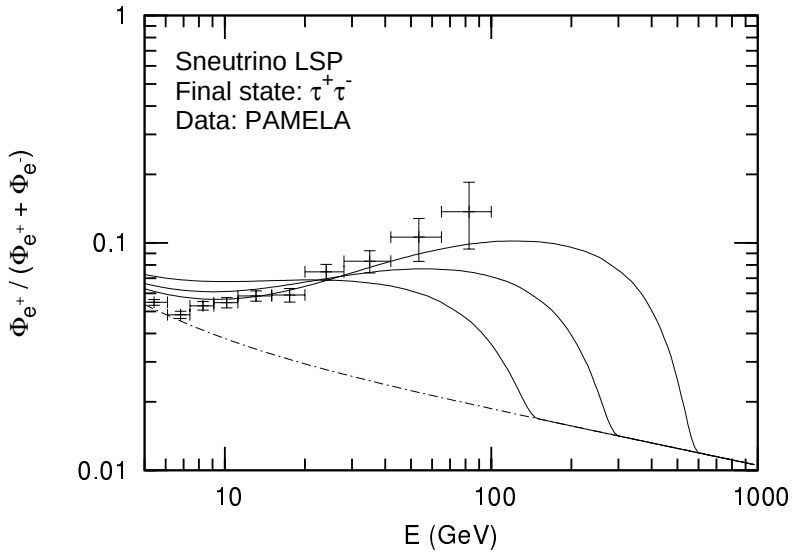

Figure 17. Same as figure 15 in the case of final state: $\tau^+\tau^-$. Here, we take $\tau_{\tilde{\nu}} = 1.8 \times 10^{26}$ sec, 1.5×10^{26} sec, and 1.1×10^{26} sec, which are the best-fit lifetime with MED model.

6 Conclusions and discussion

In this paper, we have studied the cosmic-ray fluxes from the decay of LSP dark matter, motivated by the recently reported anomalies by PAMELA and ATIC. We have introduced several types RPV operators so that the LSP becomes unstable, and calculated the fluxes of $e^{\pm}$, as well as those of $\bar{p}$, and γ-ray, assuming that the LSP is the dominant component of

JHEP05(2009)110

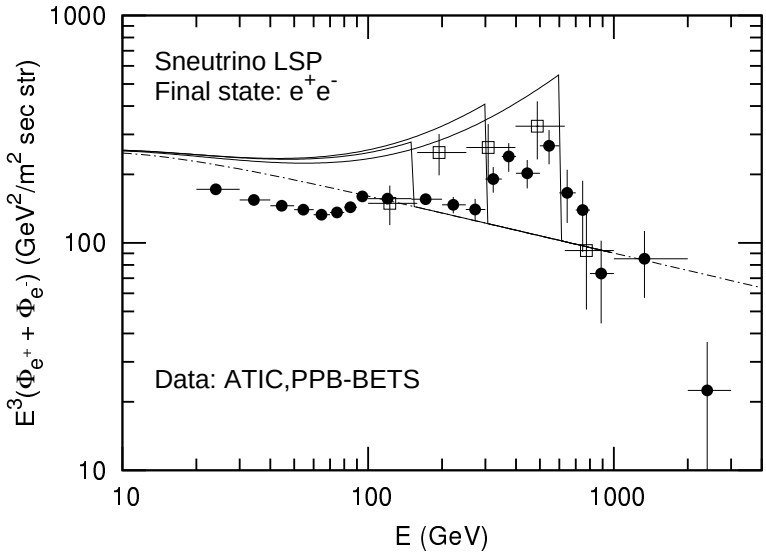

Figure 18. Total fluxes of positron and electron in MED model for the case sneutrino decays to the final state: e^+e^-. Here, we take the the same mass and lifetime as figure 15, and also take $m_{\tilde{\nu}} = 1.5\,\mathrm{TeV}$ with 1.2×10^{26} section

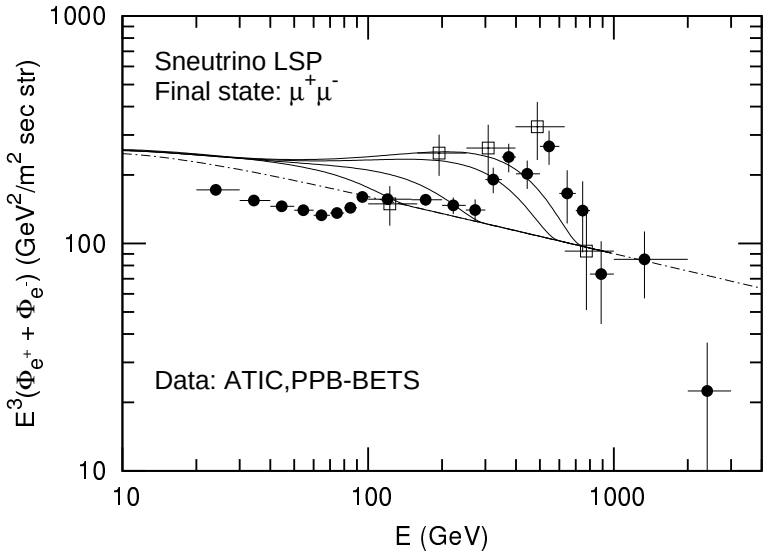

Figure 19. Same as figure 18 for the case of final state: $\mu^+\mu^-$. We take the the same mass and lifetime as figure 16.

dark matter. The detailed shape of the spectra of cosmic-ray $e^{\pm}$ depend on the properties of the LSP dark matter. However, when the lifetime of the LSP is of $O(10^{26}$ sec), the predicted positron fraction can be consistent with the observed one by PAMELA irrespective of the mass of the LSP. On the contrary, in order to explain the ATIC anomaly for the total flux

JHEP05(2009)110

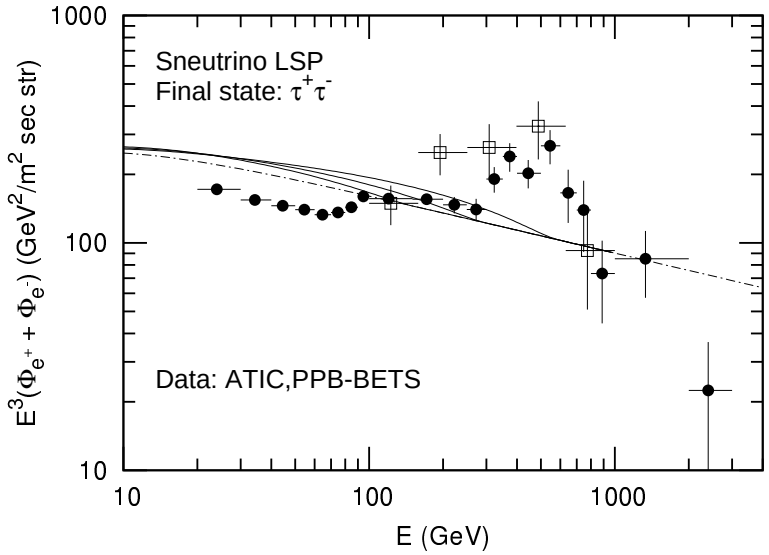

Figure 20. Same as figure 18 for the case of final state: $\tau^+\tau^-$. We take the the same mass and lifetime as figure 17.

$\Phi_{e^+} + \Phi_{e^-}$, the mass of the LSP is required to be $1-1.5$ TeV, depending on the decay modes of the LSP. If a monochromatic $e^{\pm}$ is produced by the two-body decay process, the LSP mass can be as light as ~ 1 TeV, while larger mass is required for the ATIC anomaly for other cases. In any case, in order to explain the ATIC anomaly, relatively large value of the MSSM particle masses are required, which may make it difficult to solve the naturalness problem with supersymmetry.

When the LSP decays via the bi-linear RPV interaction given in eq. (3.1), significant amount of γ and anti-proton are also produced by the decay. In particular, it has been discussed that the anti-proton flux may give a stringent constraint on the decaying dark matter scenario [46]. However, taking account of the uncertainties in the propagation models as well as the errors in the observed fluxes, we have shown that the scenarios discussed in this paper are not excluded by the present observations. In addition, we have also seen that the γ-ray flux is consistent with the currently available observational results. With improved knowledges about the propagation of the anti-proton, more detailed test of the scenario may become possible in the future. It is also notable that a precise measurement of the cosmic-ray γ flux is expected by the Fermi Telescope. Furthermore, informations about the decaying dark matter may be imprinted in the synchrotron radiation from the Galactic center [61] and in high-energy neutrino flux [62]. Future improvements of the observations of cosmic-ray fluxes should provide better understandings of the properties of dark matter.

JHEP05(2009)110

Acknowledgments

This work was supported in part by Research Fellowships of the Japan Society for the Promotion of Science for Young Scientists (K.I.), and by the Grant-in-Aid for Scientific Research from the Ministry of Education, Science, Sports, and Culture of Japan, No. 19540255 (T.M.).

A Green's function

We discuss here how we obtain the Green's function for cosmic ray positrons from the LSP decay. As mentioned in section 2, the Green's function is obtained by solving the diffusion equation (2.3) with the boundary condition $f_{e^\pm}(E, \vec{x}) = 0$ at the surface of the diffusion zone. Because of the condition, it is convenient to expand the solution by Bessel series for r (the radius of the cylinder) and Fourier series for the z (the thickness of the zone). We then find that the positron flux is obtained as

$$[\Phi_{e^\pm}]_{\rm DM} = \frac{c}{4\pi} f_{e^\pm} = \frac{c}{4\pi m_{\rm LSP}\tau_{\rm LSP}} \int_E^\infty dE' G(E, E') \left[\frac{dN_{e^\pm}}{dE'}\right]_{\rm dec}. \tag{A.1}$$

Defining the the variable

$$X(E, E') = \frac{E^{\delta-1} - (E')^{\delta-1}}{\delta - 1}, \tag{A.2}$$

the Green's function $G(E, E')$ turns out to be

$$G(E, E') = \frac{\tau}{E^2} \sum_{n=1}^{\infty}\sum_{m=0}^{\infty} I_{nm} \exp\left[\left(\frac{\zeta_n^2}{R^2} + \frac{m^2\pi^2}{4L^2}\right) K_{e^\pm}^{(0)} \tau X(E, E')\right], \tag{A.3}$$

$$\begin{aligned} I_{nm} = {} & \frac{2}{J_1^2(\zeta_n) R^2 L} J_0\left[\frac{\zeta_n}{R} r_\odot\right] \sin\left[-\frac{m\pi}{2}\right] \\ & \times \int_0^R dr \int_0^L dz\; 2r\rho_{\rm DM}(\sqrt{r^2+z^2}) J_0\left[\frac{\zeta_n}{R} r\right] \sin\left[\frac{m\pi}{2L}(z - L)\right], \end{aligned} \tag{A.4}$$

where $\tau \equiv E^2/b(E)$, J_n is the n-th order Bessel function, and ζ_n are successive zeros of J_0. The above formula is useful to calculate the Green's function, except for the region $E \simeq E'$. This is due to the exponential suppression in eq. (A.3). For the other energy region, we have checked that the summations over n and m are well converged when we take the Bessel (Fourier) series large enough.[9]

When $E \simeq E'$, the convergence becomes worse. In fact, the result is not converged for the cuspy profiles such as NFW and Moore profiles even if we take the summations up to $\mathcal{O}(1000)$. However, note that the flux for $E \simeq E'$ originates from the LSP decay in the vicinity of the solar system. Using the fact, we can express the Green's function $G(E, E')$ in another form as

$$G(E, E') = \frac{\tau}{E^2} \left[\exp\left(-K_{e^\pm}^{(0)} \tau X(E, E') \nabla^2\right) \rho_{\rm DM}(r)\right]_{r=r_\odot}. \tag{A.5}$$

[9] We have taken the summations up to $n, m = 100$ in our study.

JHEP05(2009)110

In contrast with the previous formula, this formula is valid in the region $X(E, E') \ll 1$, namely $E \simeq E'$. By matching two formulas in eqs. (A.3) and (A.5) at appropriate value of $X(E, E')$, we can obtain the Green's function numerically without wasting time for computation.

References

[1] WMAP collaboration, G. Hinshaw et al., *Five-Year Wilkinson Microwave Anisotropy Probe (WMAP1) Observations:Data processing, sky maps, & basic results*, *Astrophys. J. Suppl.* **180** (2009) 225 [arXiv:0803.0732] [SPIRES].

[2] PAMELA collaboration, O. Adriani et al., *An anomalous positron abundance in cosmic rays with energies 1.5.100 GeV*, *Nature* **458** (2009) 607 [arXiv:0810.4995] [SPIRES].

[3] J. Chang et al., *An excess of cosmic ray electrons at energies of 300.800 GeV*, *Nature* **456** (2008) 362 [SPIRES].

[4] D. Hooper, P. Blasi and P.D. Serpico, *Pulsars as the sources of high energy cosmic ray positrons*, *JCAP* **01** (2009) 025 [arXiv:0810.1527][SPIRES].

[5] Y. Nomura and J. Thaler, *Dark matter through the axion portal*, arXiv:0810.5397 [SPIRES].

[6] P.f. Yin, Q. Yuan, J. Liu, J. Zhang, X.j. Bi and S.h. Zhu, *PAMELA data and leptonically decaying dark matter*, *Phys. Rev.* **D 79** (2009) 023512 arXiv:0811.0176 [SPIRES].

[7] K. Ishiwata, S. Matsumoto and T. Moroi, *Cosmic-Ray positron from superparticle dark matter and the PAMELA anomaly*, arXiv:0811.0250 [SPIRES].

[8] Y. Bai and Z. Han, *A unified dark matter model in sUED*, arXiv:0811.0387 [SPIRES].

[9] C.-R. Chen, F. Takahashi and T.T. Yanagida, *High-energy cosmic-ray positrons from hidden-gauge-boson dark matter*, *Phys. Lett.* **B 673** (2009) 255 [arXiv:0811.0477] [SPIRES].

[10] K. Hamaguchi, E. Nakamura, S. Shirai and T.T. Yanagida, *Decaying dark matter baryons in a composite messenger model*, arXiv:0811.0737 [SPIRES].

[11] E. Ponton and L. Randall, *TeV scale singlet dark matter*, *JHEP* **04** (2009) 080 [arXiv:0811.1029] [SPIRES].

[12] A. Ibarra and D. Tran, *Decaying dark matter and the PAMELA anomaly*, *JCAP* **02** (2009) 021 [arXiv:0811.1555] [SPIRES].

[13] C.R. Chen, M.M. Nojiri, F. Takahashi and T.T. Yanagida, *Decaying hidden gauge boson and the PAMELA and ATIC/PPB-BETS anomalies*, arXiv:0811.3357 [SPIRES].

[14] A. Arvanitaki, S. Dimopoulos, S. Dubovsky, P.W. Graham, R. Harnik and S. Rajendran, *Astrophysical probes of unification*, arXiv:0812.2075 [SPIRES].

[15] K. Hamaguchi, S. Shirai and T.T. Yanagida, *Cosmic ray positron and electron excess from hidden-fermion dark matter decays*, *Phys. Lett.* **B 673** (2009) 247 arXiv:0812.2374 [SPIRES].

[16] I. Gogoladze, R. Khalid, Q. Shafi and H. Yuksel, *CMSSM spectroscopy in light of PAMELA and ATIC*, arXiv:0901.0923 [SPIRES].

[17] K. Hamaguchi, F. Takahashi and T.T. Yanagida, *Decaying gravitino dark matter and an upper bound on the gluino mass*, arXiv:0901.2168 [SPIRES].

JHEP05(2009)110

[18] E. Nardi, F. Sannino and A. Strumia, *Decaying dark matter can explain the electron/positron excesses*, *JCAP* **01** (2009) 043 [arXiv:0811.4153] [SPIRES].

[19] J.H. Huh, J.E. Kim and B. Kyae, *Two dark matter components in $N_{DM}MSSM$ and PAMELA data*, arXiv:0809.2601 [SPIRES].

[20] C.R. Chen and F. Takahashi, *Cosmic rays from leptonic dark matter*, *JCAP* **02** (2009) 004 [arXiv:0810.4110] [SPIRES].

[21] C.H. Chen, C.Q. Geng and D.V. Zhuridov, *ATIC/PAMELA anomaly from fermionic decaying dark matter*, arXiv:0901.2681 [SPIRES].

[22] M. Cirelli, M. Kadastik, M. Raidal and A. Strumia, *Model-independent implications of the e^+, e^-, anti-proton cosmic ray spectra on properties of dark matter*, *Nucl. Phys.* **B 813** (2009) 1 [arXiv:0809.2409] [SPIRES].

[23] I. Cholis, D.P. Finkbeiner, L. Goodenough and N. Weiner, *The PAMELA positron excess from annihilations into a light boson*, *Phys. Rev.* **D 79** (2009) 063509 [arXiv:0810.5344] [SPIRES].

[24] D. Feldman, Z. Liu and P. Nath, *PAMELA positron excess as a signal from the hidden sector*, arXiv:0810.5762 [SPIRES].

[25] P.J. Fox and E. Poppitz, *Leptophilic dark matter*, arXiv:0811.0399 [SPIRES].

[26] L. Bergstrom, T. Bringmann and J. Edsjo, *New positron spectral features from supersymmetric dark matter - a way to explain the PAMELA data?*, *Phys. Rev.* **D 78** (2008) 103520 [arXiv:0808.3725] [SPIRES].

[27] V. Barger, W.Y. Keung, D. Marfatia and G. Shaughnessy, *PAMELA and dark matter*, *Phys. Lett.* **B 672** (2009) 141 [arXiv:0809.0162] [SPIRES].

[28] A.E. Nelson and C. Spitzer, *Slightly non-minimal dark matter in PAMELA and ATIC*, arXiv:0810.5167 [SPIRES].

[29] R. Harnik and G.D. Kribs, *An effective theory of dirac dark datter*, arXiv:0810.5557 [SPIRES].

[30] J. Hisano, M. Kawasaki, K. Kohri, T. Moroi and K. Nakayama, *Cosmic Rays from dark matter annihilation and big-bang nucleosynthesis*, arXiv:0901.3582 [SPIRES].

[31] M. Ibe, H. Murayama and T.T. Yanagida, *Breit-wigner enhancement of dark matter annihilation*, arXiv:0812.0072 [SPIRES].

[32] J. Hisano, S. Matsumoto and M.M. Nojiri, *Explosive dark matter annihilation*, *Phys. Rev. Lett.* **92** (2004) 031303 [hep-ph/0307216] [SPIRES];
J. Hisano, S. Matsumoto, M.M. Nojiri and O. Saito, *Non-perturbative effect on dark matter annihilation and gamma ray signature from galactic center*, *Phys. Rev.* **D 71** (2005) 063528 [hep-ph/0412403] [SPIRES];
J. Hisano, S. Matsumoto, O. Saito and M. Senami, *Heavy Wino-like neutralino dark matter annihilation into antiparticles*, *Phys. Rev.* **D 73** (2006) 055004 [hep-ph/0511118] [SPIRES];
N. Arkani-Hamed, D.P. Finkbeiner, T. Slatyer and N. Weiner, *A theory of dark matter*, *Phys. Rev.* **D 79** (2009) 015014 [arXiv:0810.0713] [SPIRES].

[33] D. Hooper, A. Stebbins and K.M. Zurek, *The PAMELA and ATIC excesses from a Nearby Clump of neutralino dark matter*, arXiv:0812.3202 [SPIRES].

[34] F. Takayama and M. Yamaguchi, *Gravitino dark matter without R-parity*, *Phys. Lett.* **B 485** (2000) 388 [hep-ph/0005214] [SPIRES].

JHEP05(2009)110

[35] T. Sjostrand, S. Mrenna and P. Skands, *PYTHIA 6.4 physics and manual*, *JHEP* **05** (2006) 026 [hep-ph/0603175] [SPIRES].

[36] T. Moroi and L. Randall, *Wino cold dark matter from anomaly-mediated SUSY breaking*, *Nucl. Phys.* **B 570** (2000) 455 [hep-ph/9906527] [SPIRES].

[37] J.F. Navarro, C.S. Frenk and S.D.M. White, *A universal density profile from hierarchical clustering*, *Astrophys. J.* **490** (1997) 493 [astro-ph/9611107] [SPIRES].

[38] T. Delahaye, R. Lineros, F. Donato, N. Fornengo and P. Salati, *Positrons from dark matter annihilation in the galactic halo: theoretical uncertainties*, *Phys. Rev.* **D 77** (2008) 063527 [arXiv:0712.2312] [SPIRES].

[39] E.A. Baltz and J. Edsjo, *Positron propagation and fluxes from neutralino annihilation in the halo*, *Phys. Rev.* **D 59** (1999) 023511 [astro-ph/9808243] [SPIRES].

[40] L.C. Tan and L.K. Ng, *Calculation of the equilibrium anti-proton spectrum*, *J. Phys.* **G 9** (1983) 227 [SPIRES].

[41] R.J. Protheroe, *Cosmic ray anti-protons in the closed galaxy model*, *Astrophys. J.* **251** (1981) 387 [SPIRES].

[42] EGRET Collaboration, P. Sreekumar et al., *EGRET observations of the extragalactic gamma ray emission*, *Astrophys. J.* **494** (1998) 523 [astro-ph/9709257] [SPIRES].

[43] K. Ishiwata, S. Matsumoto and T. Moroi, work in progress.

[44] K. Ishiwata, S. Matsumoto and T. Moroi, *High energy cosmic rays from the decay of gravitino dark matter*, *Phys. Rev.* **D 78** (2008) 063505 [arXiv:0805.1133] [SPIRES].

[45] W. Buchmuller, L. Covi, K. Hamaguchi, A. Ibarra and T. Yanagida, *Gravitino dark matter in R-parity breaking vacua*, *JHEP* **03** (2007) 037 [hep-ph/0702184] [SPIRES].

[46] A. Ibarra and D. Tran, *Antimatter signatures of gravitino dark matter decay*, *JCAP* **07** (2008) 002 [arXiv:0804.4596] [SPIRES].

[47] S. Torii *et al.*, *High-energy electron observations by PPB-BETS flight in antarctica*, arXiv:0809.0760 [SPIRES].

[48] G. Bertone, M. Cirelli, A. Strumia and M. Taoso, *Gamma-ray and radio tests of the $e^{\pm}$ excess from DM annihilations*, *JCAP* **03** (2009) 009 [arXiv:0811.3744] [SPIRES].

[49] H.E.S.S. Collaboration, F. Aharonian et al., *HESS observations of the galactic center region and their possible dark matter interpretation*, *Phys. Rev. Lett.* **97** (2006) 221102 [*Erratum ibid.* **97** (2006) 249901] [astro-ph/0610509] [SPIRES].

[50] T. Porter, *First results from Fermi Gamma-Ray Space Telescope*, talk given at *First results from Fermi Gamma-Ray space telescope*, Tokyo Tech, Tokyo Japan March 7 (2009) http://www.hp.phys.titech.ac.jp/fermi.

[51] S. Colafrancesco, S. Profumo and P. Ullio, *Multi-frequency analysis of neutralino dark matter annihilations in the Coma cluster*, *Astron. Astrophys.* **455** (2006) 21 [astro-ph/0507575] [SPIRES].

[52] O. Adriani et al., *A new measurement of the antiproton-to-proton flux ratio up to 100 GeV in the cosmic radiation*, *Phys. Rev. Lett.* **102** (2009) 051101 [arXiv:0810.4994] [SPIRES].

[53] T. Sanuki et al., *Precise measurement of cosmic-ray proton and helium spectra with the BESS spectrometer*, *Astrophys. J.* **545** (2000) 1135 [astro-ph/0002481] [SPIRES].

JHEP05(2009)110

[54] WIZARD collaboration, M. Boezio et al., *The cosmic ray proton and helium spectra between 0.2-GeV and 200-GeV*, *Astrophys. J.* **518** (1999) 457 [SPIRES].

[55] BESS collaboration, S. Orito et al., *Precision measurement of cosmic-ray antiproton spectrum*, *Phys. Rev. Lett.* **84** (2000) 1078 [astro-ph/9906426] [SPIRES];
Y. Asaoka et al., *Measurements of cosmic-ray low-energy antiproton and proton spectra in a transient period of the solar field reversal*, *Phys. Rev. Lett.* **88** (2002) 051101 [astro-ph/0109007] [SPIRES];
K. Abe et al., *Measurement of cosmic-ray low-energy antiproton spectrum with the first BESS-polar antarctic flight*, *Phys. Lett.* **B 670** (2008) 103 [arXiv:0805.1754] [SPIRES].

[56] WIZARD/CAPRICE collaboration, M. Boezio et al., *The cosmic-ray anti-proton flux between 3-GeV and 49-GeV*, *Astrophys. J.* **561** (2001) 787 [astro-ph/0103513] [SPIRES].

[57] K. Ishiwata, T. Ito and T. Moroi, *Long-lived unstable superparticles at the LHC*, *Phys. Lett.* **B 669** (2008) 28 [arXiv:0807.0975] [SPIRES].

[58] T. Falk, K.A. Olive and M. Srednicki, *Heavy sneutrinos as dark matter*, *Phys. Lett.* **B 339** (1994) 248 [hep-ph/9409270] [SPIRES].

[59] L.J. Hall, T. Moroi and H. Murayama, *Sneutrino cold dark matter with lepton-number violation*, *Phys. Lett.* **B 424** (1998) 305 [hep-ph/9712515] [SPIRES].

[60] T. Asaka, K. Ishiwata and T. Moroi, *Right-handed sneutrino as cold dark matter*, *Phys. Rev.* **D 73** (2006) 051301 [hep-ph/0512118] [SPIRES].

[61] K. Ishiwata, S. Matsumoto and T. Moroi, *Synchrotron radiation from the galactic center in decaying dark matter scenario*, *Phys. Rev.* **D 79** (2009) 043527 [arXiv:0811.4492] [SPIRES].

[62] J. Hisano, M. Kawasaki, K. Kohri and K. Nakayama, *Neutrino signals from annihilating/decaying dark matter in the light of recent measurements of cosmic ray electron/positron fluxes*, arXiv:0812.0219 [SPIRES].

JHEP05(2009)110

Received: *June 19, 2009*

Erratum

Eq. (4.6) should be:

$$\frac{d\Gamma_{\tilde{B}\to\nu_i l^{\pm}_{L,j} l^{\mp}_{R,k}}}{dE_{l_L} dE_{l_R}} = \frac{g_1^2 \lambda_{ijk}^2}{64\pi^3 m_{\tilde{B}}} \frac{z_{l_R}(1-z_{l_R})}{[(m_{\tilde{l}_{R,k}}/m_{\tilde{B}})^2 - 1 + z_{l_R}]^2}, \tag{B.1}$$

JHEP05(2009)110